US009417216B2

(12) **United States Patent**
Kim et al.

(10) **Patent No.: US 9,417,216 B2**
(45) **Date of Patent: Aug. 16, 2016**

(54) **ATOMIC LAYER DEPOSITION INVERTED PASSIVATED SURFACE ACOUSTIC WAVE SENSOR FOR EARLY DETECTION OF BIOFILM GROWTH**

(71) Applicant: **University of Maryland**, College Park, MD (US)

(72) Inventors: **Young Wook Kim**, Seoul (KR); **Reza Ghodssi**, Potomac, MD (US); **Agisilaos A. Iliadis**, Edgewater, MD (US); **William E. Bentley**, Annapolis, MD (US); **Mariana Tsacoumis Meyer**, Baltimore, MD (US)

(73) Assignee: **University of Maryland**, College Park, MD (US)

(*) Notice: Subject to any disclaimer, the term of this patent is extended or adjusted under 35 U.S.C. 154(b) by 31 days.

(21) Appl. No.: **14/157,094**

(22) Filed: **Jan. 16, 2014**

(65) **Prior Publication Data**

US 2014/0199757 A1 Jul. 17, 2014

Related U.S. Application Data

(60) Provisional application No. 61/753,332, filed on Jan. 16, 2013.

(51) **Int. Cl.**

C12M 1/34	(2006.01)
G01N 29/28	(2006.01)
G01N 29/02	(2006.01)
G01N 29/036	(2006.01)

(52) **U.S. Cl.**

CPC ***G01N 29/28*** (2013.01); ***G01N 29/022*** (2013.01); ***G01N 29/036*** (2013.01); *G01N 2291/0256* (2013.01); *G01N 2291/0258* (2013.01); *G01N 2291/0423* (2013.01)

(58) **Field of Classification Search**

CPC G01N 2291/0256; G01N 2291/0423; G01N 29/022; G01N 2291/0255; G01N 29/036; G01N 29/2437; G01N 29/28; G01N 33/54373; B01L 2400/0436; B01L 3/502707; B01L 3/50273

See application file for complete search history.

(56) **References Cited**

PUBLICATIONS

Kim et al,"A Bacterial Biofilm Surface Acoustic Wave Sensor for Real Time Biofilm Growth Monitoring", IEEE Sensors Nov. 1-4, 2010 Conference, pp. 1568-1571.*

Kim et al,"An ALD aluminum oxide passivated Surface Acoustic Wave sensor for early biofilm detection" Sensors and Actuators B 163 (published online Jan. 16, 2012) 136-145.*

(Continued)

Primary Examiner — Dennis M White

(74) *Attorney, Agent, or Firm* — Carter, DeLuca, Farrell & Schmidt, LLP

(57) **ABSTRACT**

A surface acoustic wave (SAW) biofilm sensor includes a transmitting electric to acoustic wave transducer defining an upper surface and a lower surface, a receiving acoustic wave to electric transducer defining an upper surface and a lower surface, a piezoelectric film layer defining an upper surface and a lower surface, and a passivation film layer defining an upper surface and a lower surface. Portions of the lower surface of the piezoelectric film layer are disposed on the upper surface of the transmitting electric to acoustic wave transducer and on the upper surface of the receiving acoustic wave to electric transducer, and the lower surface of the passivation film layer is disposed on the upper surface of the piezoelectric film layer such that the upper surface of the passivation film layer is configured to enable contact with a biofilm.

39 Claims, 26 Drawing Sheets

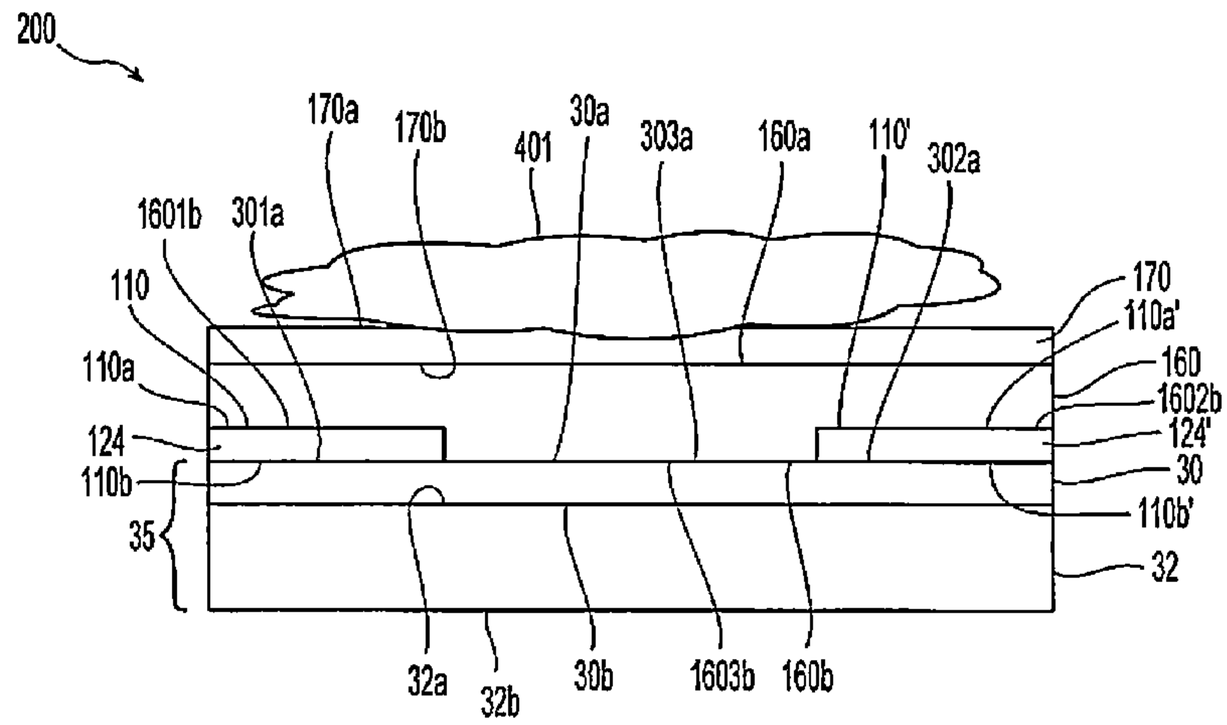

(56) **References Cited**

PUBLICATIONS

Kim, "An atomic layer deposition passivated Surface Acoustic Wave sensor for bacterial biofilm growth monitoring", Dissertation, University of Maryland, College Park, First publically available Apr. 4, 2013.*

J. W. Costerton et al., Bacterial Biofilms: A Common Cause of Persistent Infections, Science, vol. 284, (1999), p. 1318-1322.

Sutherland, I. W., Bacterial exopolysaccharides—their nature and production, Surface Carbohydrates of the Prokaryotic Cell, London, Academic Press, (1977), p. 27-96.

J. W. Costerton, et al., Bacterial Biofilms in Nature and Disease, Annu. Rev. Microbiol, 41, (1987), p. 435-506.

Liju Yang, et al., Detection of viable *Salmonella* using microelectrode-based capacitance measurement coupled with immunomagnetic separation, Journal of Microbiological Methods, 64, (2006), p. 9-16.

Ebrahim Ghafar-Zadeh, et al., Bacteria Growth Monitoring Through a Differential CMOS Capacitive Sensor, IEEE Transactions on Biomedical Circuits and Systems, vol. 4, No. 4, (2010), p. 232-238.

X. Munoz-Berbel, et al., Impedimetric approach for quantifying low bacteria concentrations based on the changes produced in the electrode-solution interface during the pre-attachment stage, Biosensors and Bioelectronics., 23, (2008), p. 1540-1546.

E. Spiller, et al., A sensitive microsystem as biosensor for cell growth monitoring and antibiotic testing, Sensors and Actuators A, 130-131, (2006), p. 312-321.

Ewa Heyduk, et al., Fluorescent homogeneous immunosensors for detecting pathogenic bacteria, Analytical Biochemistry, (2010), p. 396, 298-303.

Benjamin J. Privett, et al., Electrochemical Sensors, Anal. Chem., (2010), 82, p. 4723-4741.

Michiel van Leeuwen, et al., Aerobic Batch Cultivation in Micro Bioreactor with Integrated Electrochemical Sensor Array, Biotechnol. Prog., vol. 26, No. 1, (2010), p. 293-300.

G. L. Harding, et al., Love wave acoustic immunosensor operating in liquid, Sensors and Actuators A, 61, (1997), p. 279-286.

J. Du, et al., A study of Love-wave acoustic sensors, Sensors and Actuators A, 56, (1996), p. 211-219.

J. Du, et al., An experimental study of Love-wave acoustic sensors operating in liquids, Sensors and Actuators A, 60, (1997), p. 54-61.

K. Z. Kourosh, et al., Novel Love mode surface acoustic wave based immunosensors, Sensor and Actuators B, 91, (2003), p. 143-147.

S. Krishnamoorthy, et al., Properties of high sensitivity ZnO surface acoustic wave sensors on SiO2/(100) Si substrates, Solid-State Electronics, 52, (2008), p. 1710-1716.

H. Morkoc, et al., Zinc Oxide: Fundamentals, Materials and Device Technology (Chapter 1: General Properties of ZnO), Wiley-VCH Verag GmbH, Weinheim, 2009.

R. D. Vispute et al., High quality crystalline ZnO buffer layers on sapphire (001) by pulsed laser deposition for III-V nitrides, Applied Physics Letters 70 2735 (1997), p. 2735-2737.

S. Krishnamoorthy, et al., Development of high frequency ZnO/SiO2/Si Love mode surface acoustic wave devices, Solid-State Electronics, 50, (2006), p. 1113-1118.

S. Krishnamoorthy, et al., An interleukin-6 ZnO/SiO2/Si surface acoustic wave biosensor, Biosensors and Bioelectronics, 24, (2008), p. 313-318.

M. C. Horrillo et al., Optimization of SAW sensors with a structure ZnO—SiO2—Si to detect volatile organic compounds, Sensors and Actuators B, 118, (2006), p. 356-361.

X. Chen, D. Liu, Temperature stability of ZnO-based Love wave biosensor with SiO2 buffer layer, Sens. Actuat. A, 156, (2009), p. 317-322.

X. Chen, D. Liu, J. Chen, G. Wang, The effect of a SiO2 layer on the performance of a ZnO-based SAW device for high sensitivity biosensor applications, Smart Mater. Struct. 18, (2009), 115021 (8 pp).

A. Springer, R. Weigel, A. Pohl, F. Seifert, Wireless identification and sensing using surface acoustic wave devices, IEEE ASME Trans Mechatron, 9,(1999), p. 745-756.

Alfred Pohl, A Review of Wireless SAW Sensors, IEEE Transactions on Ultrasonics, Ferroelectrics and Frequency Control, vol. 47, No. 2, (Mar. 2000), p. 317-332.

Arruda David L, Wilson William C, Nguyen Crystal, Yao Qi W, Caiazzo Robert, Talpasanu Ilie, Dow Douglas, Liu Brian, Microelectrical sensors as emerging platforms for protein biomaker detection in point-of-care diagnostics, Expert Rev. Mol. Diagn., vol. 9, No. 7, (2009), p. 749-755.

M. Bisoffi, B. Hjelle, D.C. Brown, D.W. Branch, T.L. Edwards, S.M. Brozik, V.S. Bondu-Hawkins, R. S. Larson, Detection of viral bioagents using a shear horizontal surface acoustic wave biosensor, Biosensors & Bioelectronics, 23, (2008), pp. 1397-1403.

Y.Q.Fu, J.K. Luo, X.Y. Du, A.J. Flewitt, Y. Li, G.H. Markx, A.J. Walton, W.I. Milne, Recent developments on ZnO films for acoustic wave bio-sensing and microfluidic applications: a review, Sensors and Actuators B-CHEM, 143, (2010), p. 606-619.

Irie RF, Natural antibody in human serum to neoantigen in human cultured cells grown in fetal bovine serum, J. Natl Cancer Inst, 52(4), (1974), p. 1051-1058.

Glen McHale, Generalized concept of shear horizontal acoustic plate mode and Love wave sensors, Institute of physics publishing, Meas. Sci Technol. 14, (2003), p. 1847-1853.

Biljana A. Cavic, Gordon L. Hayward, and Michael Thompson, Acoustic waves and the study of biochemical macromolecules and cells at the sensor-liquid interface, The Analyst, 124, (1999), p. 1405-1420.

Bill Drafts, Acoustic Wave Technology Sensors, IEEE Transactions on Microwave Theory and Techniques, vol. 49, No. 4, (2001), p. 795-802.

Federal Communications Commission, Title 47 C.F.R., Chapter I, Subchapter D, Part 95, Subpart I, paragraph 1209, "Permissible communications", 77 FR 55733, as amended through Sep. 11, 2012.

Douglas H. Lowndes, D.B. Geohegan, A.A. Puretzky, D.P. Norton, C. M. Rouleau, Synthesis of Novel Thin-Film Materials by Pulsed Laser Deposition, Science, vol. 273, (1996), p. 898-903.

Susan E. Voss and Jont B. Allen, Measurement of acoustic impedance and reflectance in the human ear canal, J. Acoust. Soc. Am, 95 (1), (1994), p. 372-384.

B. Jakoby, M.J. Vellekoop, Properties of Love waves: applications in sensors, Smart Mater. Struct. 6, (1997), p. 668-679.

J. Su, Z. B. Kuang, H. Liu, Love wave in ZnO/SiO2/Si structure with initial stresses, Journal of Sound and Vibration, 286, (2005), p. 981-999.

R. C. Chang, S. Y. Chu, C. S. Hong, Y. T. Chuang, A study of Love wave devices in ZnO/Quartz and ZnO/LitaO3 structures, Thin Soild Films, 498, (2006), 146-151.

W. C. Shih, H. Y. Su, M. S. Wu, Deposition of ZnO thin films on SiO2/Si substrate with Al2O3 buffer layer by radio frequency magnetron sputtering for high frequency surface acoustic wave devices, Thin Solid Films, 517, (2009), p. 3378-3381.

W. C. Shih, T. L. Wang, L. L. Hsu, Surface acoustic wave properties of aluminum oxide films on lithium niobate, Thin Soild Films, 518, (2010), p. 7143-7146.

J. Du, G. L. Harding, A multilayer structure for Love-mode acoustic sensors, Sensors and Actuator A, 65, (1998), p. 152-159.

NIST Property Data Summaries, http://www.ceramics.nist.gov/srd/summary/emodox00.htm.

Lenntech B.V., http://www.lenntech.com/teflon.htm, c. 1998-2014.

Hang-Ju Ko, Myung-Soo Han, Young-Sik Park, Yun-Sik Yu, Byoung-In Kim, Sang Sub Kim, Jin-Hyeok Kim, Improvement of the quality of ZnO substrates by annealing, Journal of Crystal Growth, 269, (2004), p. 493-498.

Siu, Louis "Mass of a Bacterium", The Physics Factbook, Elert, Glenn ed., pp. 1-2, http://hypertextbook.com/facts/2003/LouisSiu.shtml, 2003.

Jeffrey V. Straight and Doraiswami Ramkrishna, Modeling of Bacterial Growth under Multiply-Limiting Conditions. Experiments under Carbon- or/and Nitrogen-Limiting Conditions, Biotechnol. Prog. 10, (1994), p. 588-605.

Augustin J.C et al., Significance of Inoculum Size in the Lag Time of Listeria monocytogenes, Appl. Envion. Microbiol. vol. 66, (2000), p. 1706-1710.

(56) **References Cited**

OTHER PUBLICATIONS

Mariana T Meyer, Varnika Roy, William E Bentley, and Reza Ghodssi, Development and validation of a microfluidic reactor for biofilm monitoring via optical methods, J. Micromech. Microeng., 21, (2011), 054023 (10 pp).
Federal Communications Commission, Title 47 C.F.R., Chapter I, Subchapter D, Part 95, Subpart E, paragraph 627 , "MedRadio transmitters in the 401-406 MHz band", as amended through 77 FR 4268, Jan. 27, 2012.
Federal Communications Commission, Title 47 C.F.R., Chapter I, Subchapter D, Part 95, Subpart I, paragraph 1209, "Permissible communications", 79 FR 60100, as amended through Oct. 6, 2014.
Sutherland. Bacterial exopolysaccharides—their nature and production. Antibiotics and chemotherapy 1989; 42:50-55.

* cited by examiner

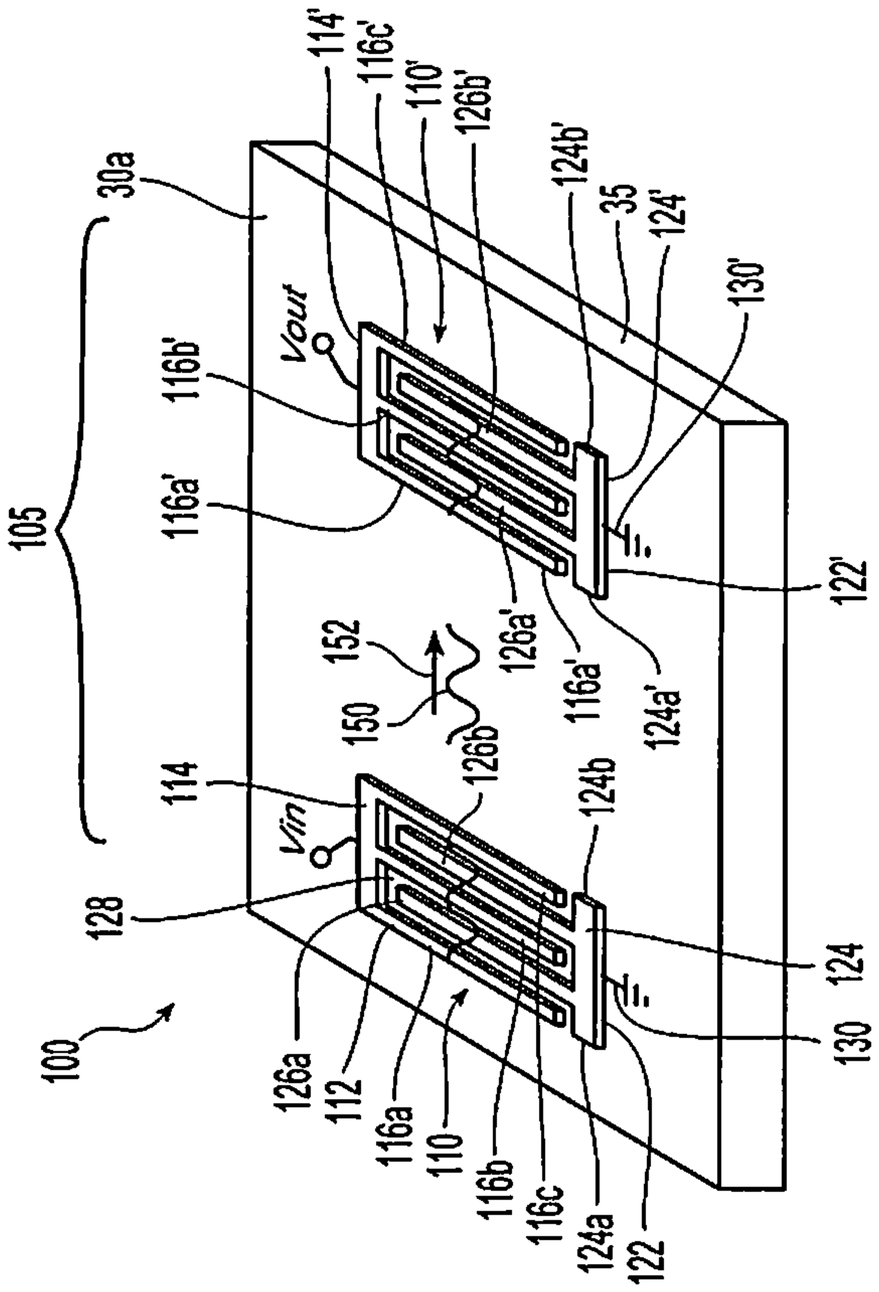
114'
116c'
110'
126b'
124b'
35
124'
130'
30a
Vout
116b'
116a'
105
122'
126a'
116a'
124a'
152
150
126b
114
124b
Vin
128
124
130
100
126a
112
116a
110
116b
116c
124a
122

Fig. 2

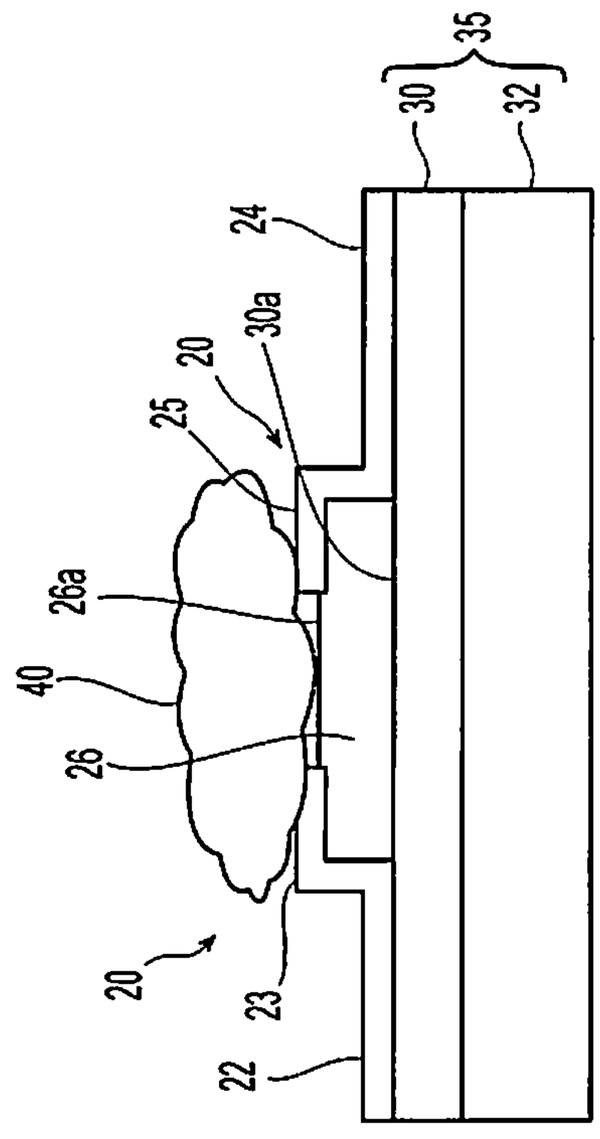
35
30
32
24
30a
20
25
26a
40
26
20
23
22

Fig. 1

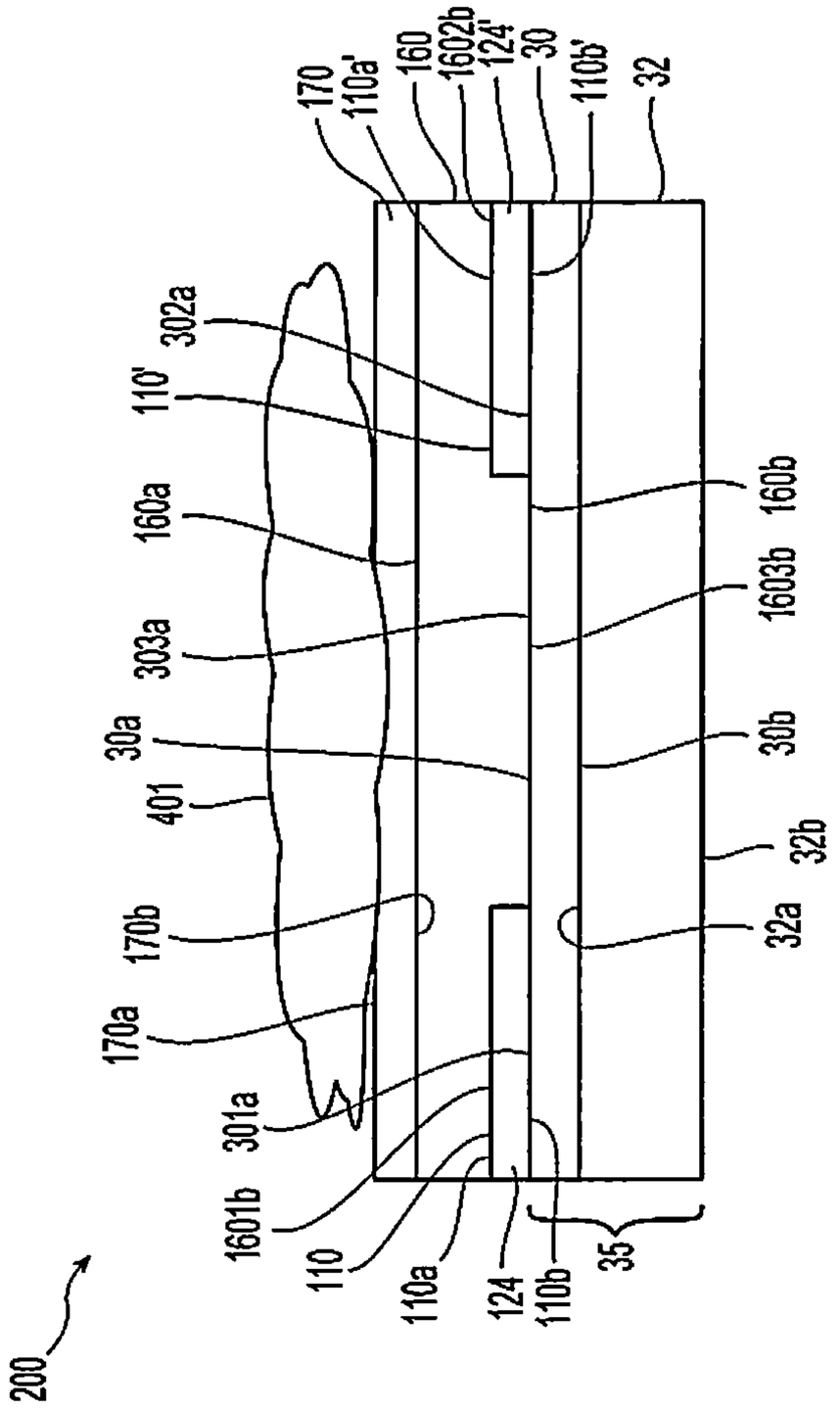
200
170
110a'
160
1602b
124'
30
110b'
32
302a
110'
160a
303a
30a
401
170b
170a
301a
1601b
110
110a
124
110b
35
160b
1603b
30b
32b
32a

Fig. 3

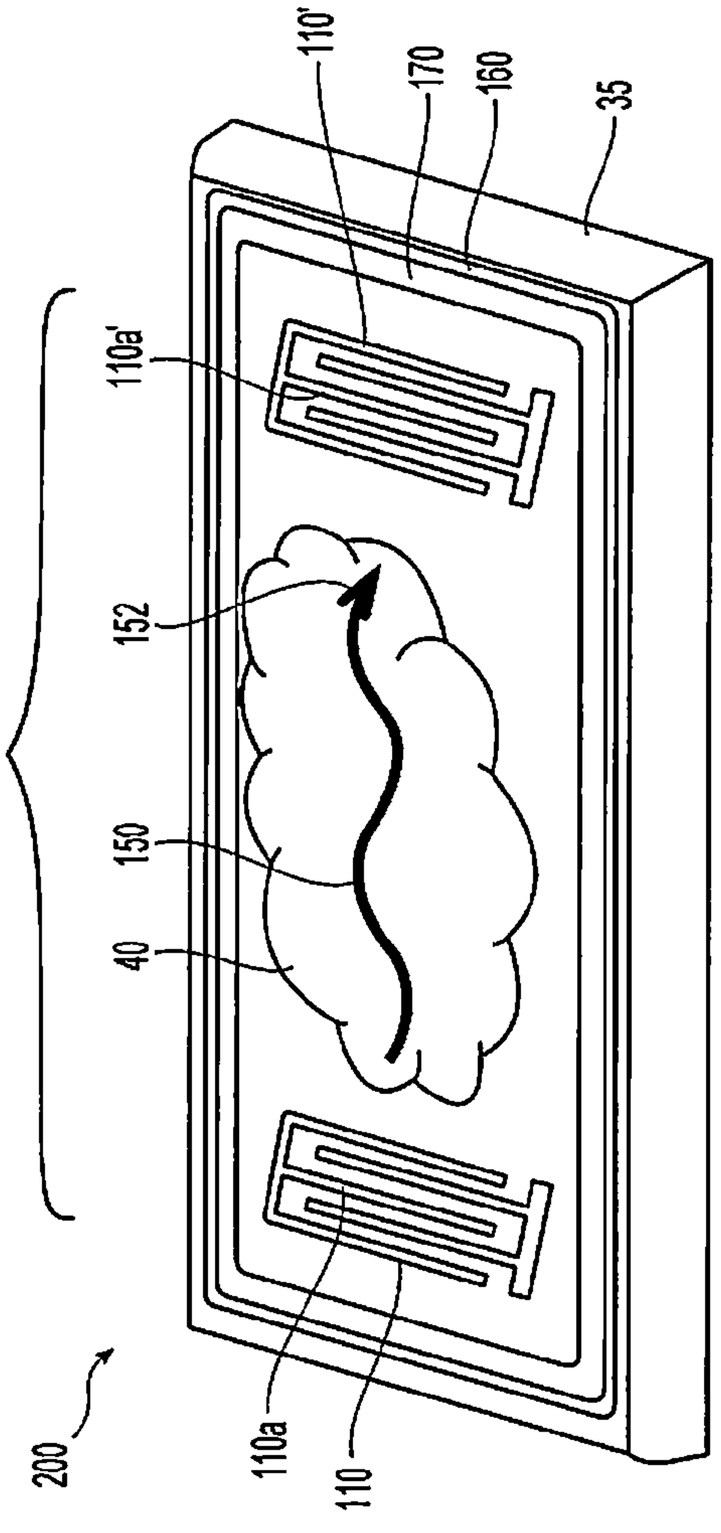
110'
170
160
35
110a'
152
105
150
40
200
110a
110

Fig. 4A

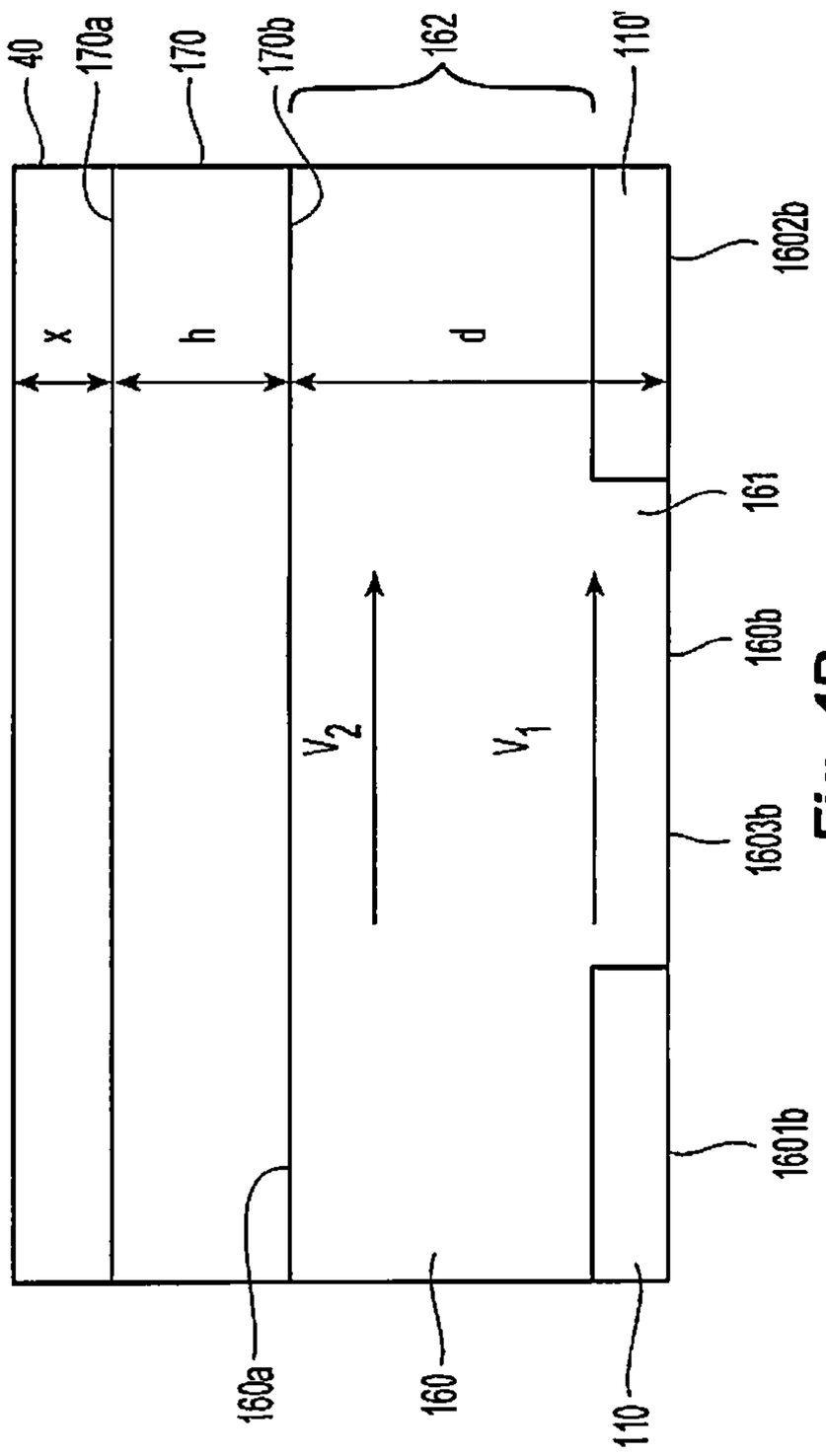
40
170a
170
170b
162
110'
1602b
x
h
d
161
160b
V_2
V_1
1603b
1601b
160a
160
110

Fig. 4B

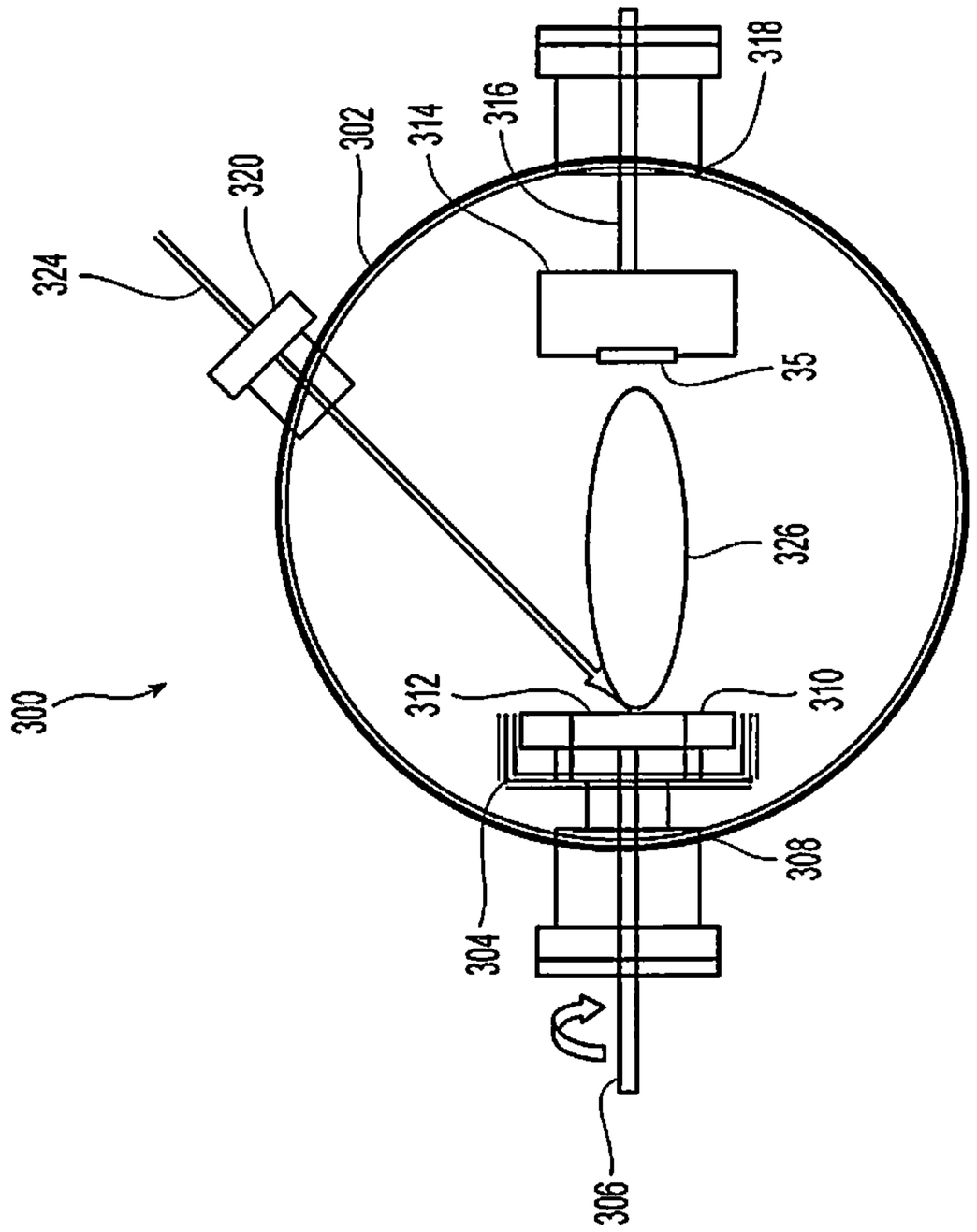

Fig. 5

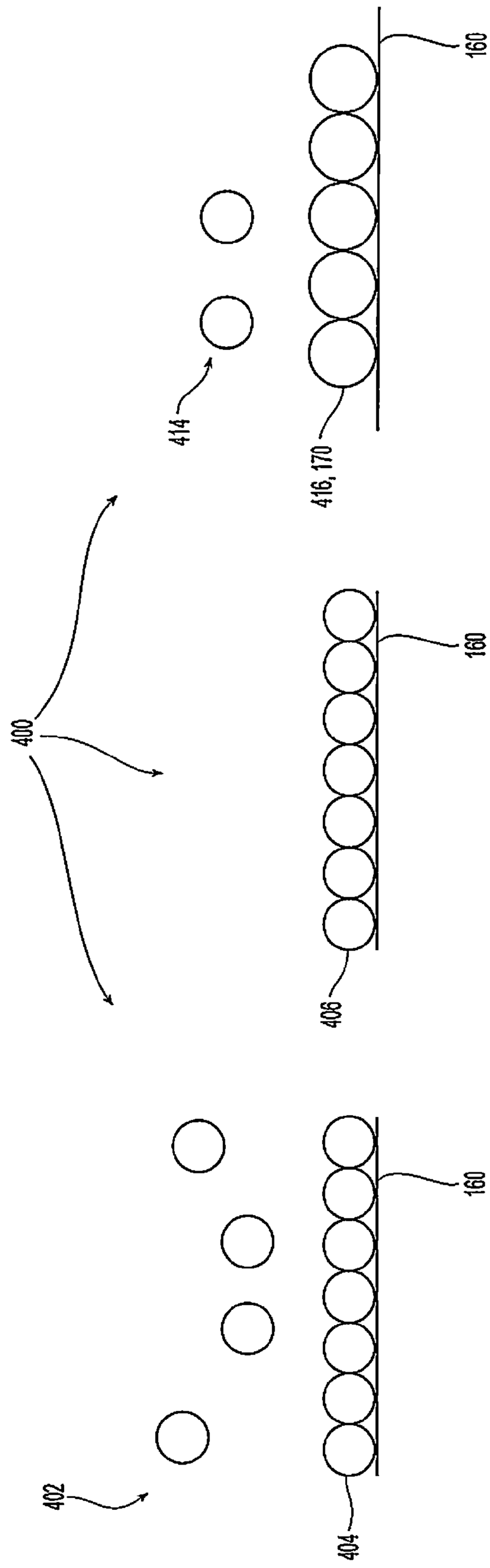

Fig. 6

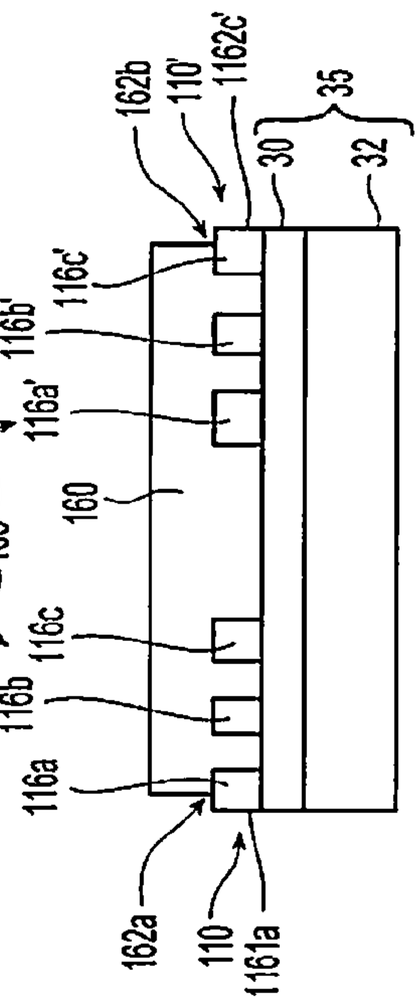

Fig. 7D

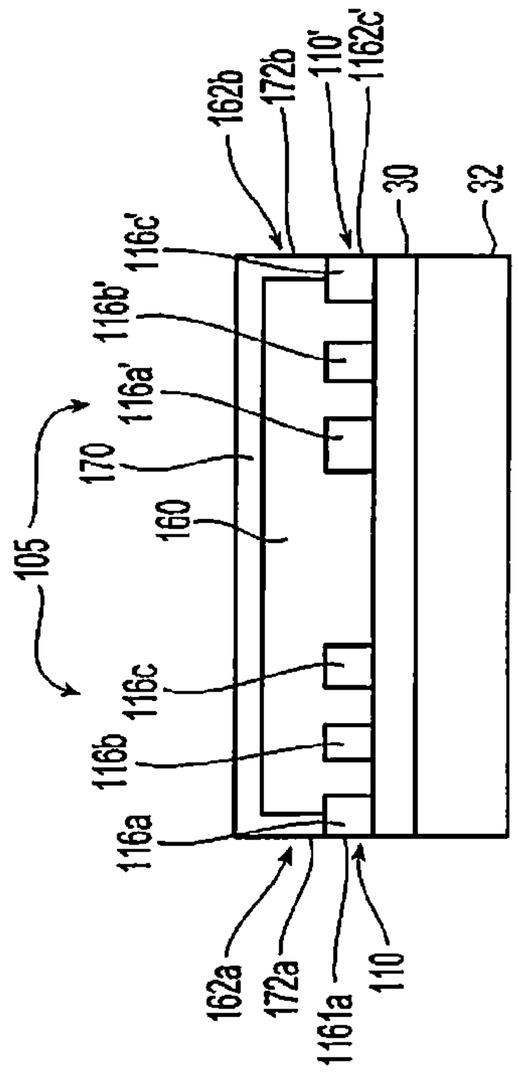

Fig. 7E

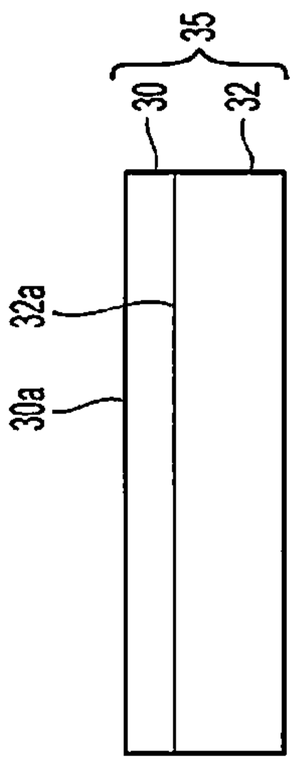

Fig. 7A

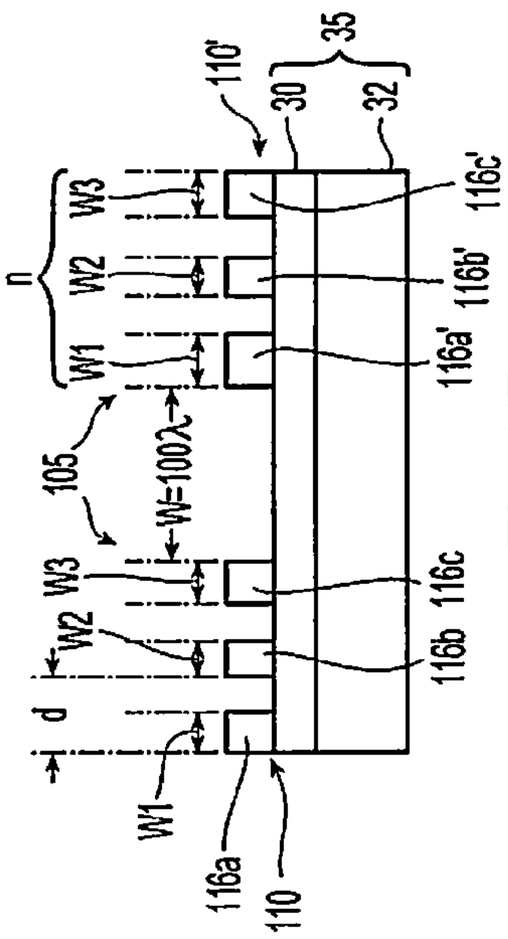

Fig. 7B

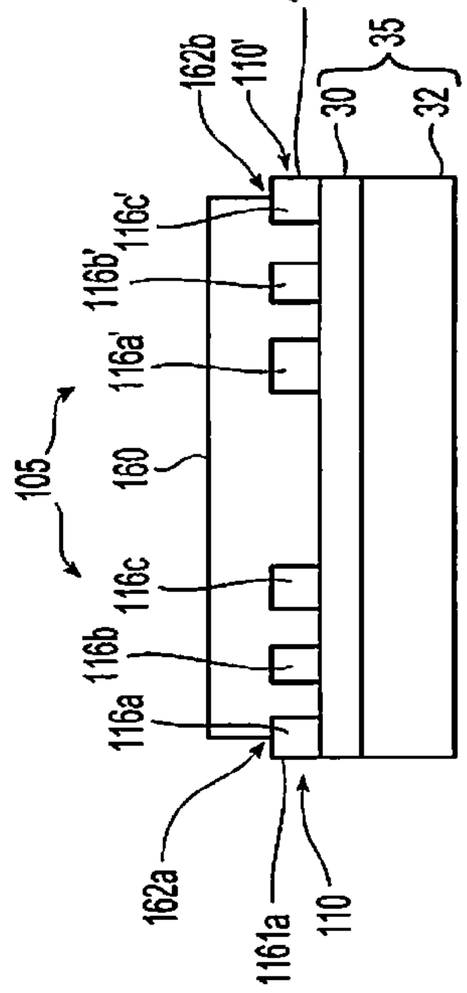

Fig. 7C

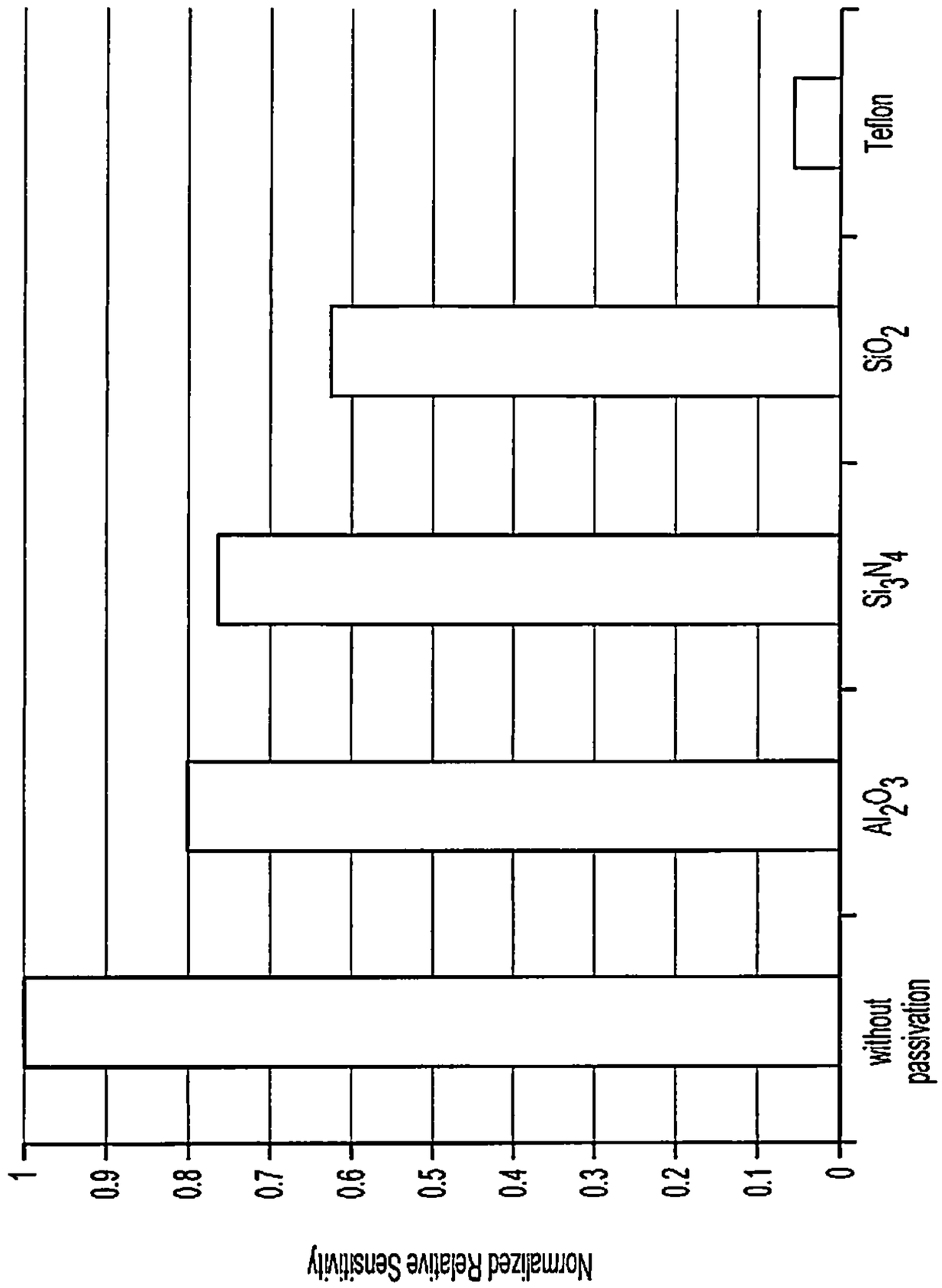
Teflon
SiO_2
Si_3N_4
Al_2O_3
without passivation
1
0.9
0.8
0.7
0.6
0.5
0.4
0.3
0.2
0.1
0
Normalized Relative Sensitivity

Fig. 8

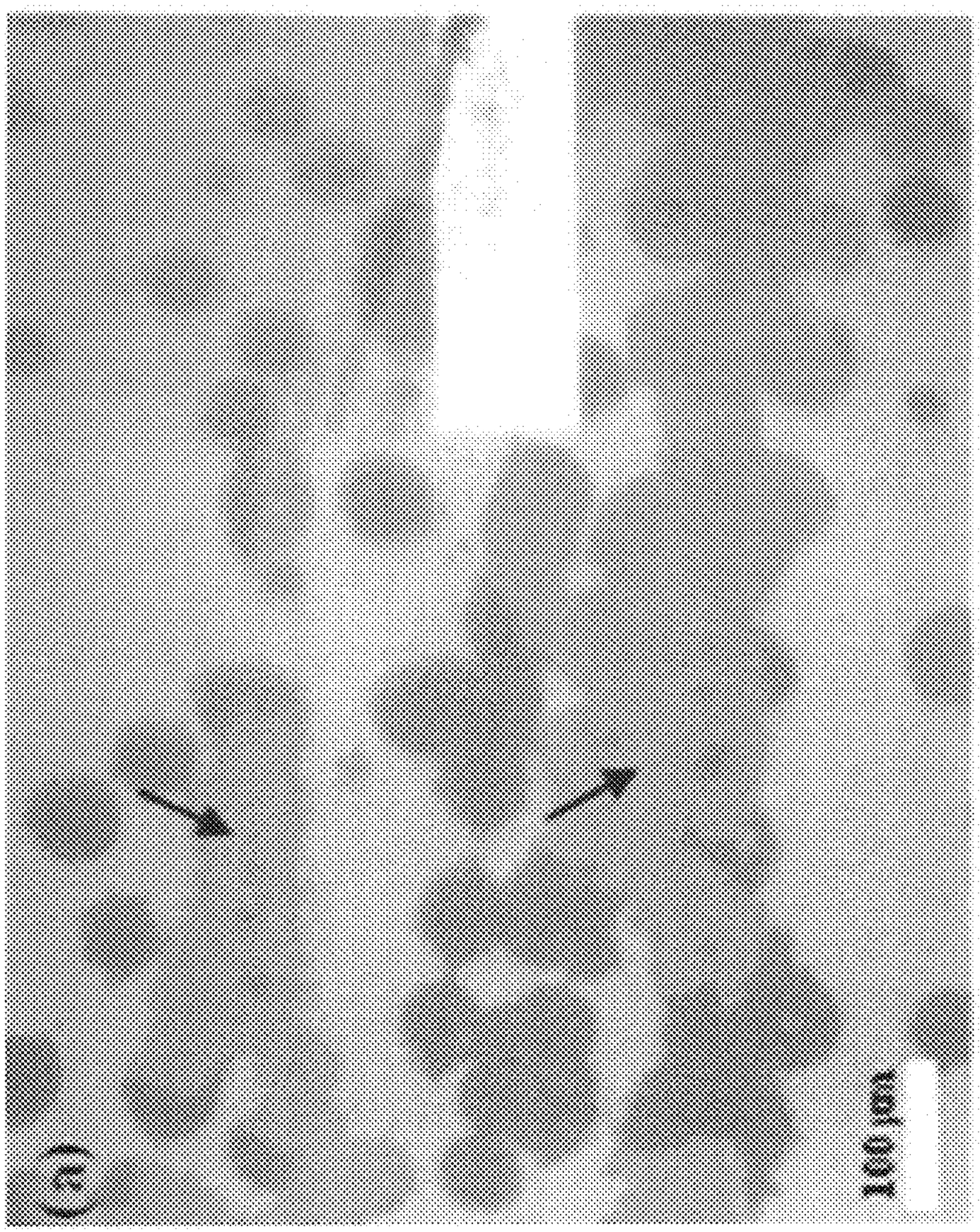
(a)
100 nm
20 nm ALD Al_2O_3 film passivation in LB media after 2 days

Fig. 9

30 nm ALD Al_2O_3 film passivation in LB media after 2 days
100 μm

Fig. 10

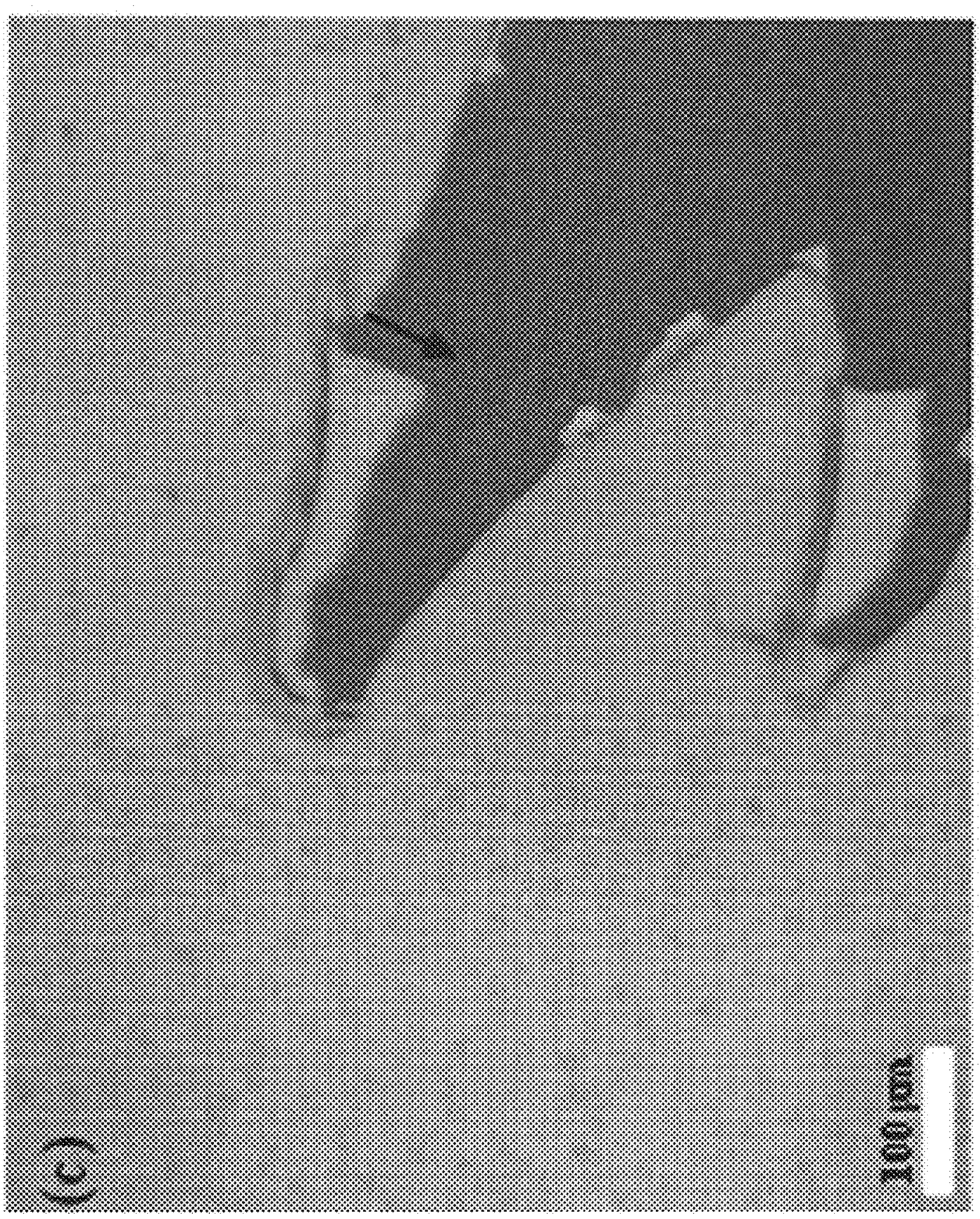
40 nm ALD Al_2O_3 film passivation in LB media after 2 days
100 nm

Fig. 11

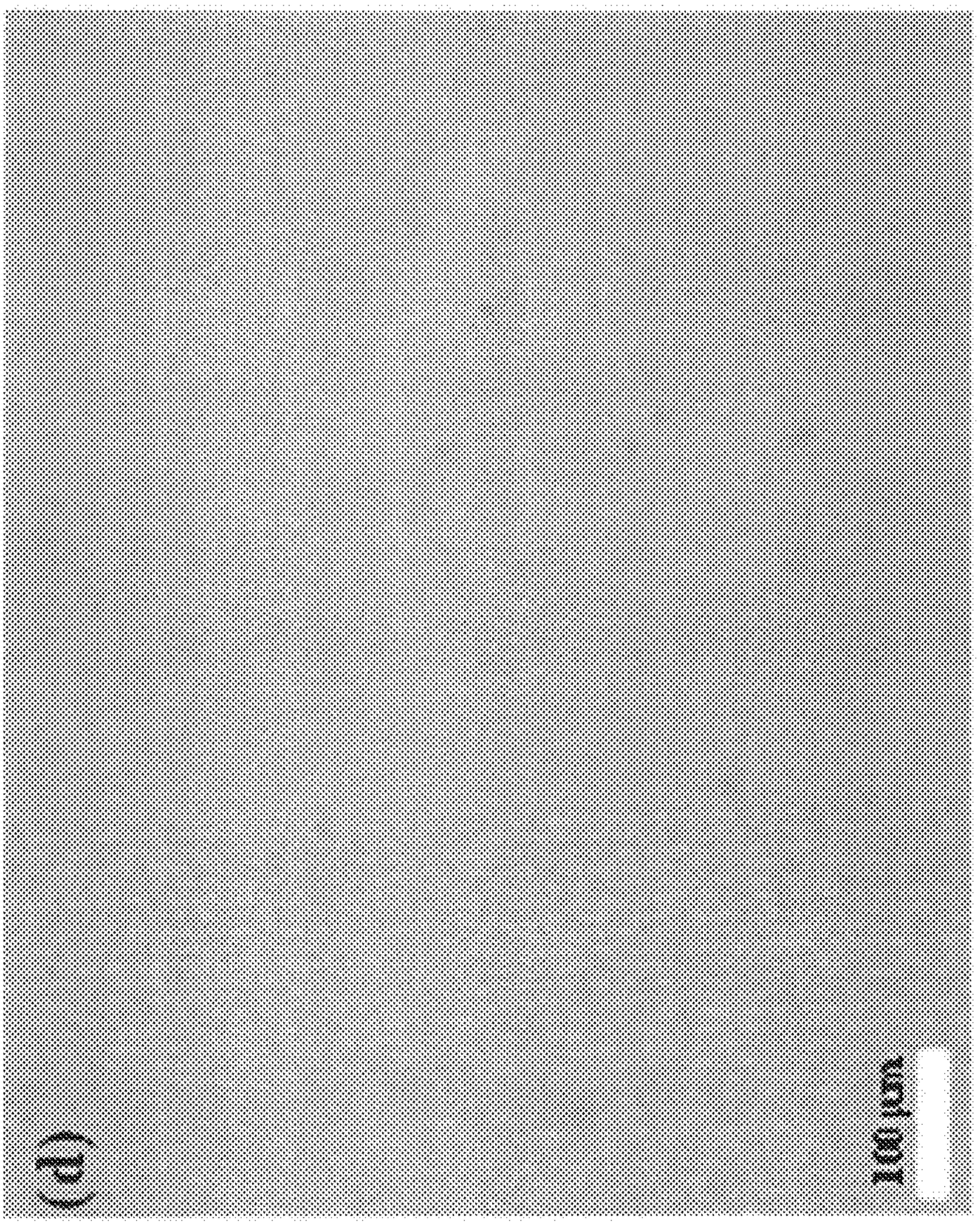
100 nm
(c)
45 nm ALD Al_2O_3 film passivation in LB media after 7 days

Fig. 12

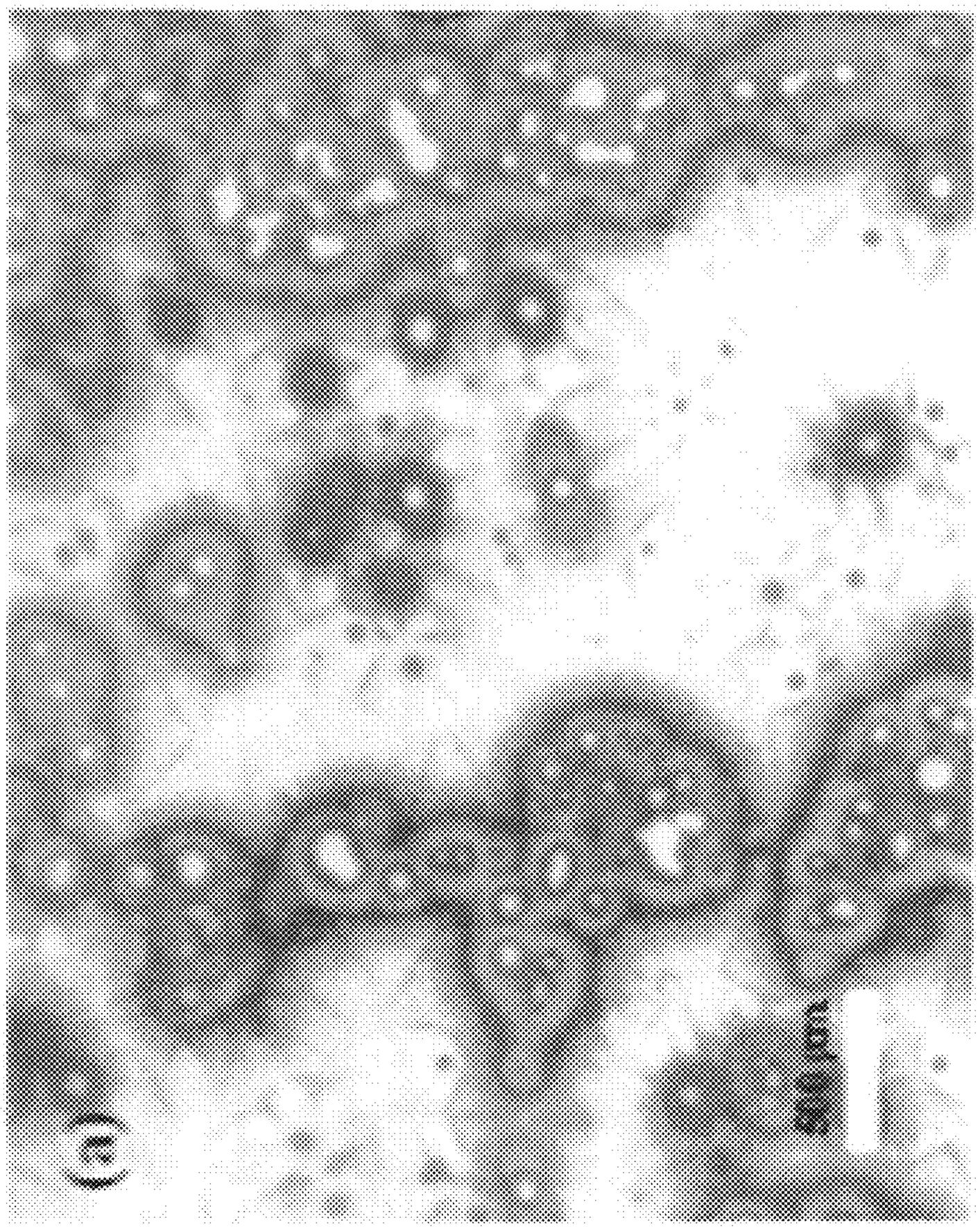
Fig. 13

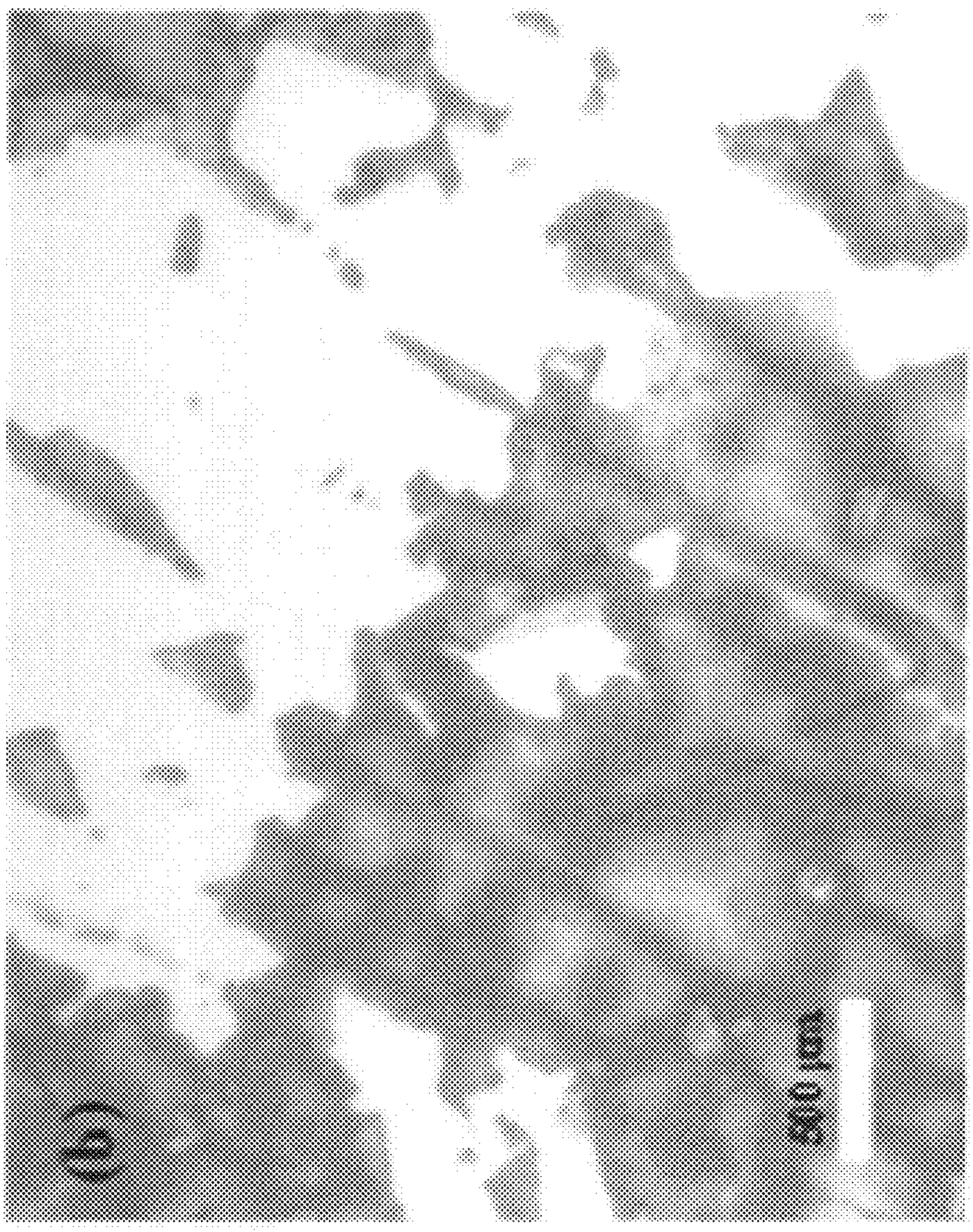

Fig. 14

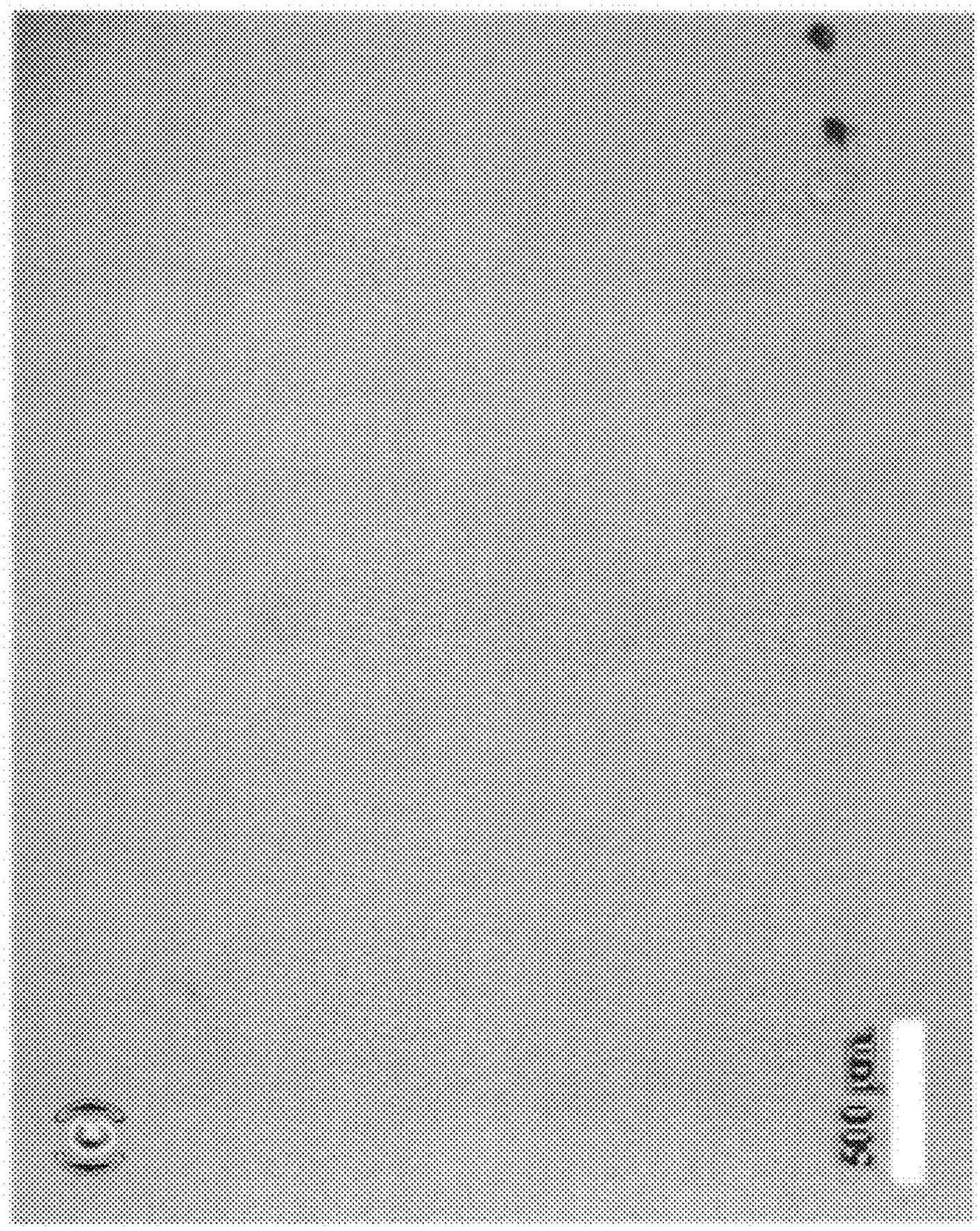
Fig. 15
Wet Mass
Dry Mass

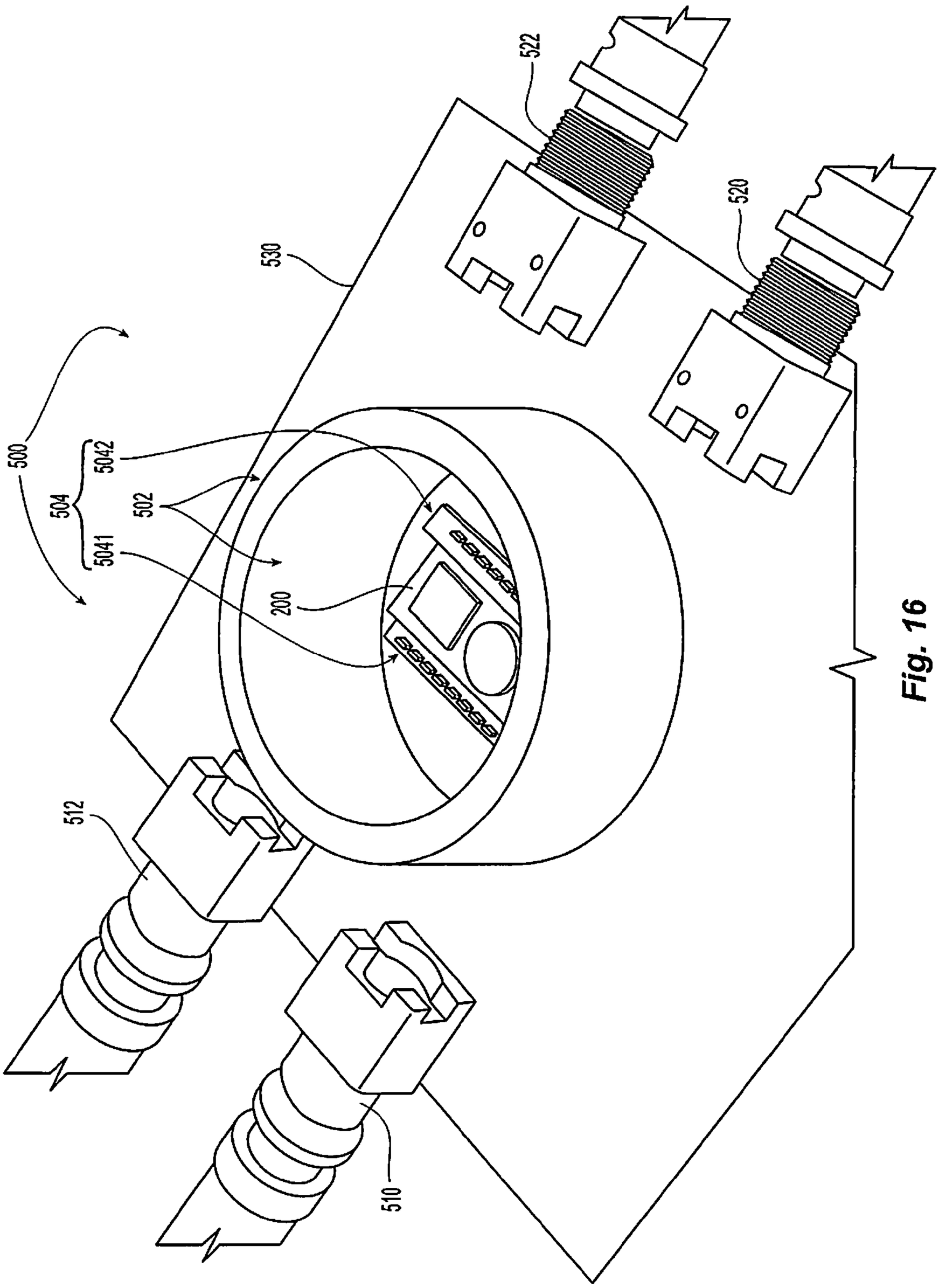

Fig. 16

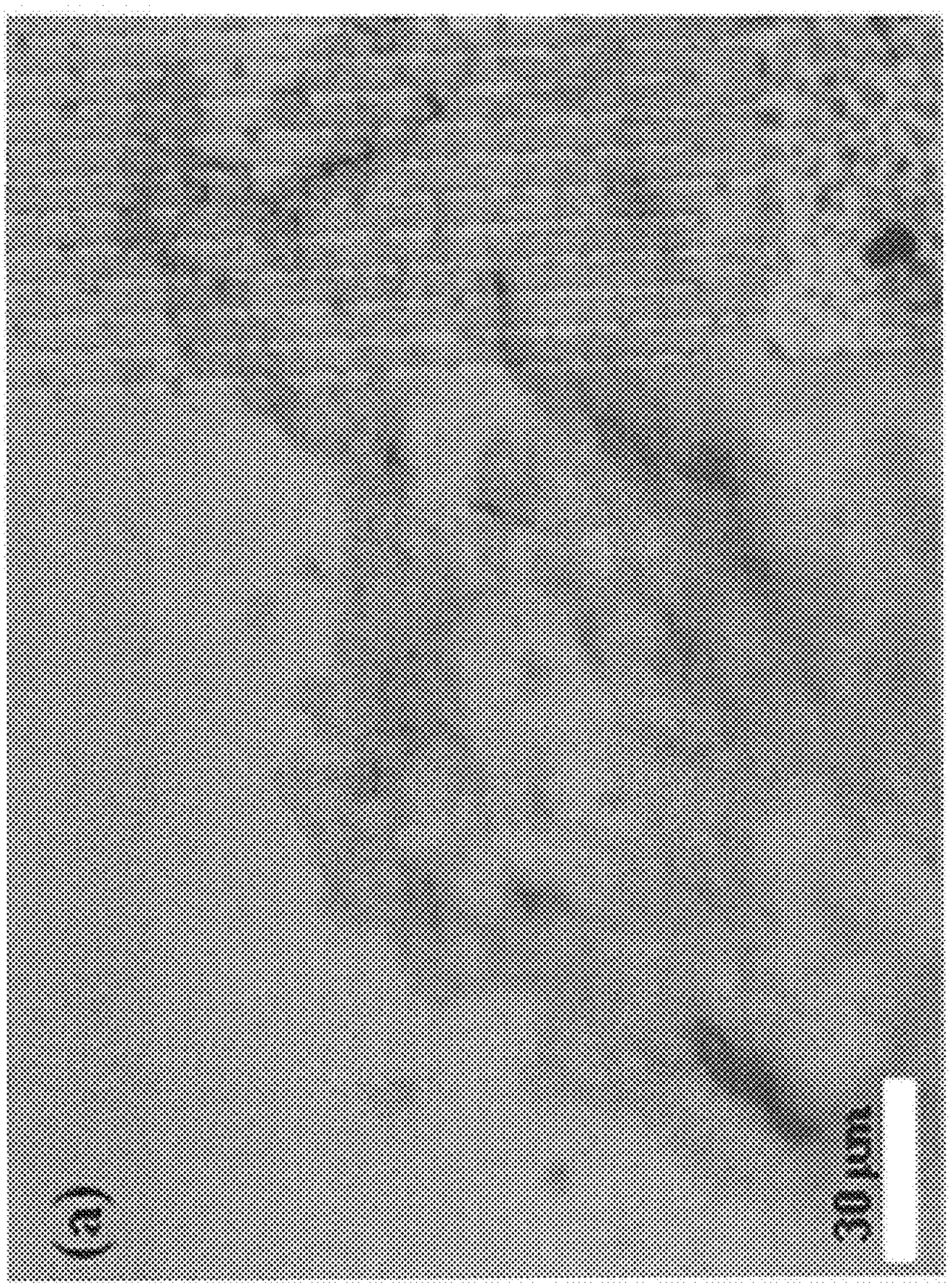

Fig. 17

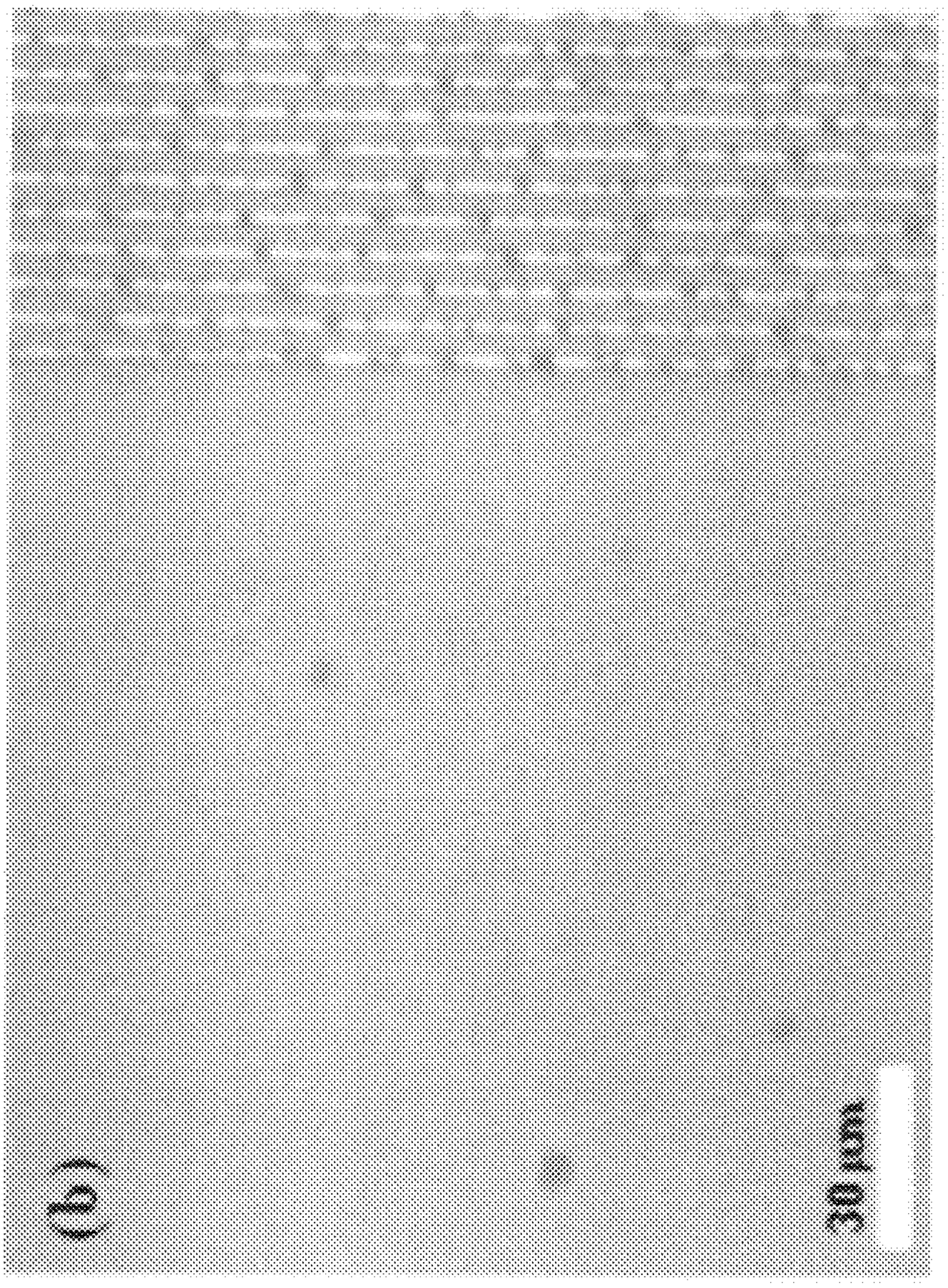

Fig. 18

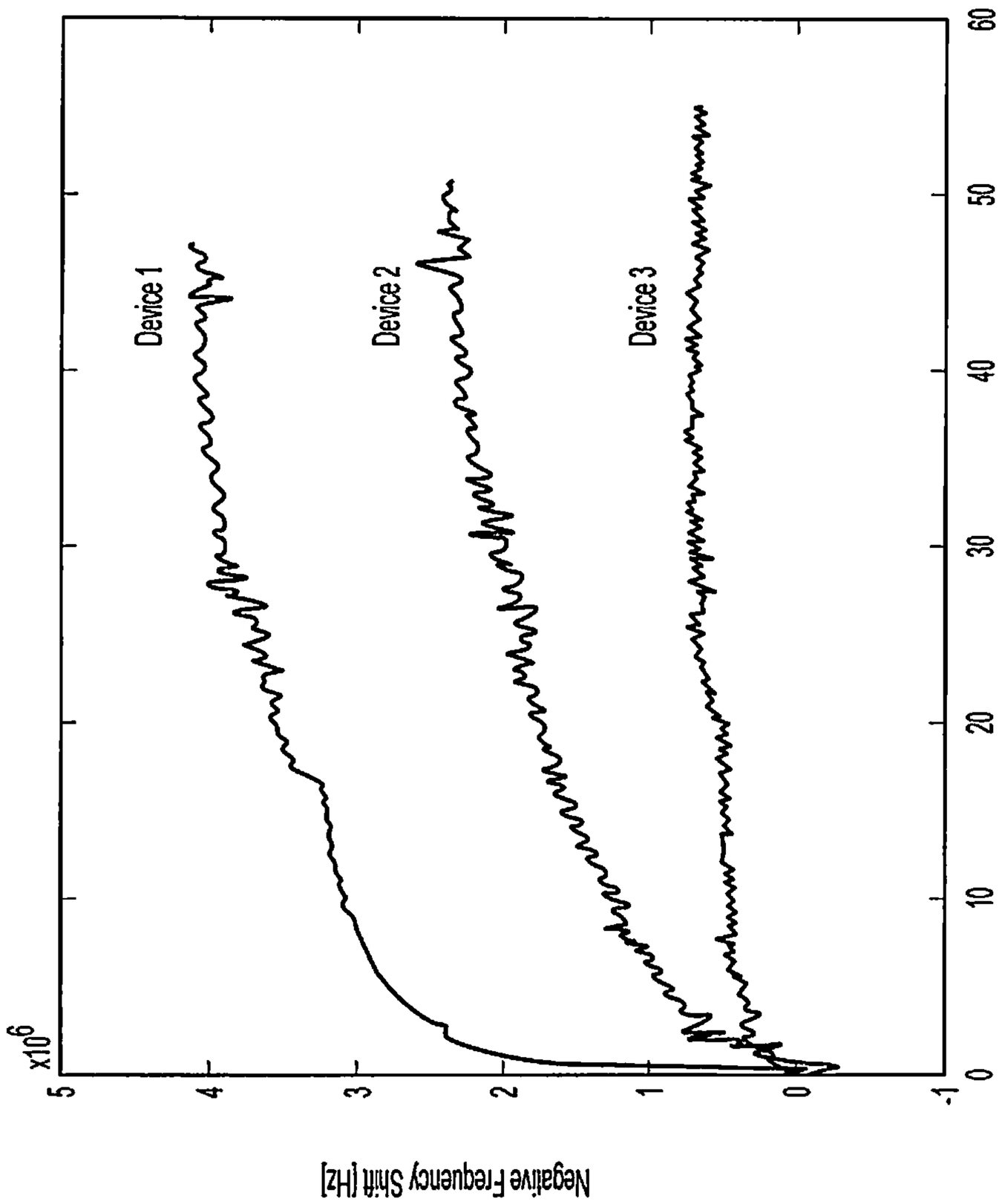
Device 1
Device 2
Device 3
Negative Frequency Shift [Hz]
x10^6
5
4
3
2
1
0
-1
0
10
20
30
40
50
60
Time [hour]

Fig. 19

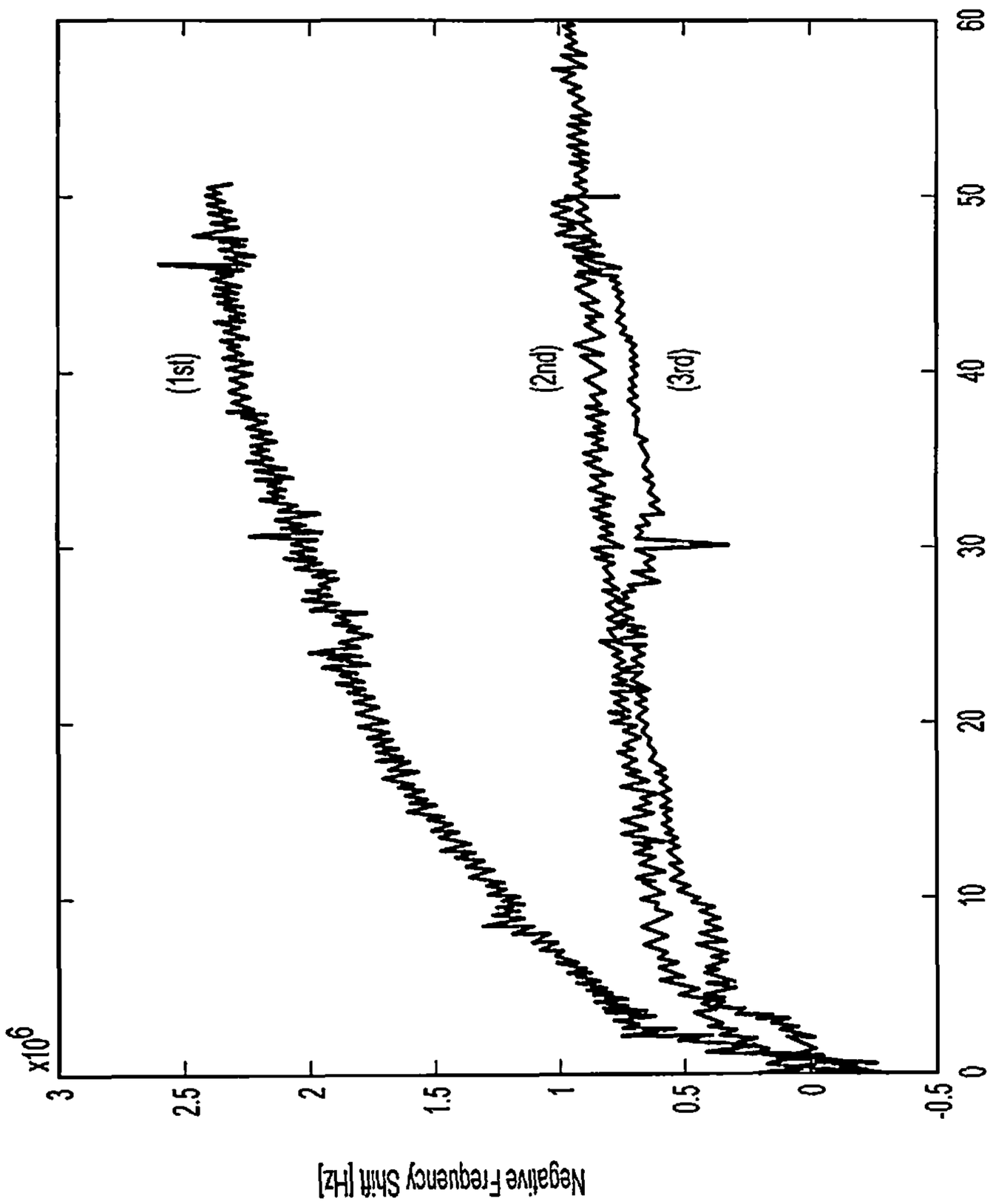
(1st)
(2nd)
(3rd)
Time [hour]
Negative Frequency Shift [Hz]
x10^6
3
2.5
2
1.5
1
0.5
0
-0.5
0
10
20
30
40
50
60

Fig. 20

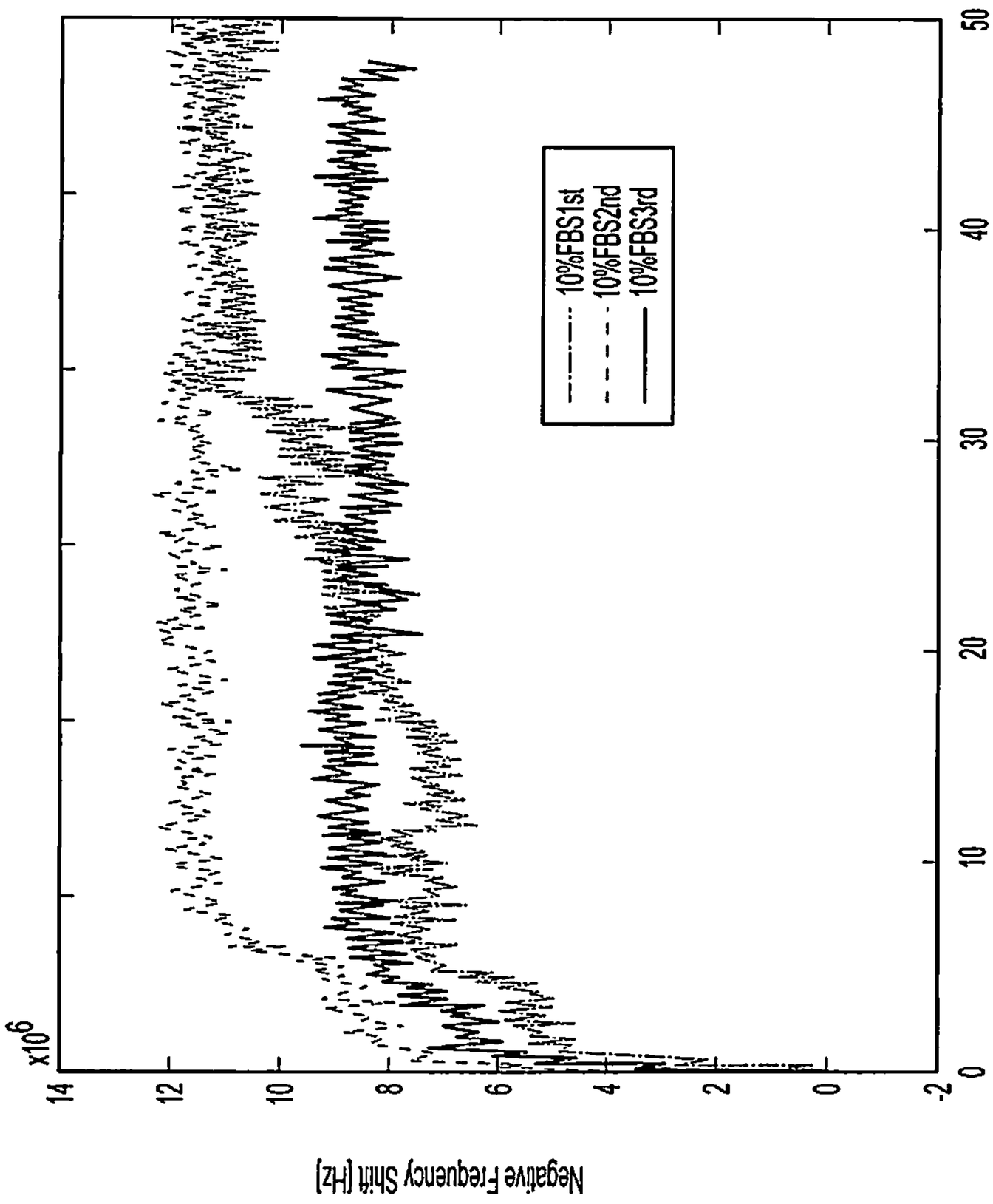
Negative Frequency Shift [Hz]
x10^6
14
12
10
8
6
4
2
0
-2
0
10
20
30
40
50
Time [hour]
10%FBS1st
10%FBS2nd
10%FBS3rd

Fig. 21

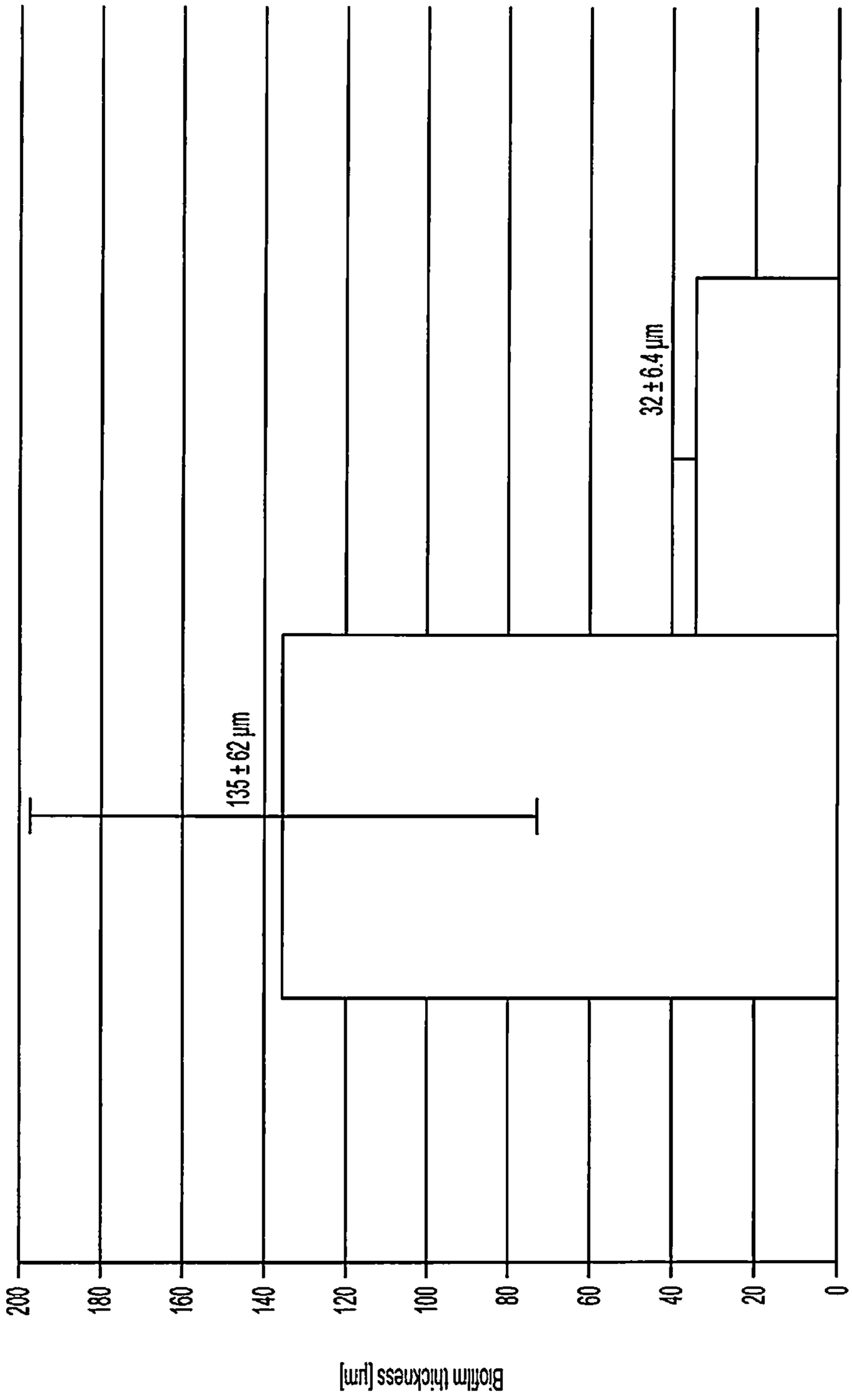
Biofilm thickness [µm]
200
180
160
140
120
100
80
60
40
20
0
LB
10% FBS
135 ± 62 µm
32 ± 6.4 µm

Fig. 22

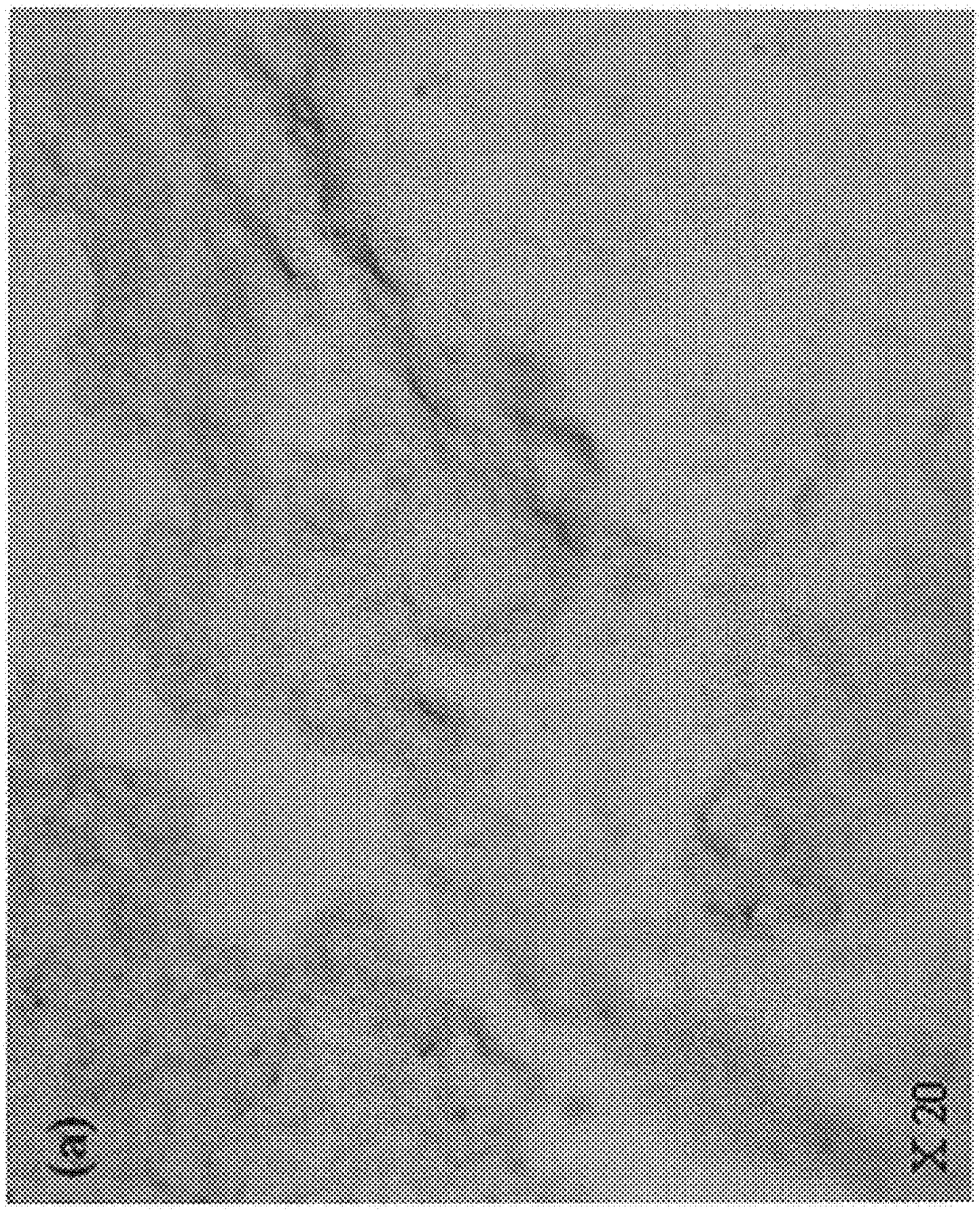

Fig. 23

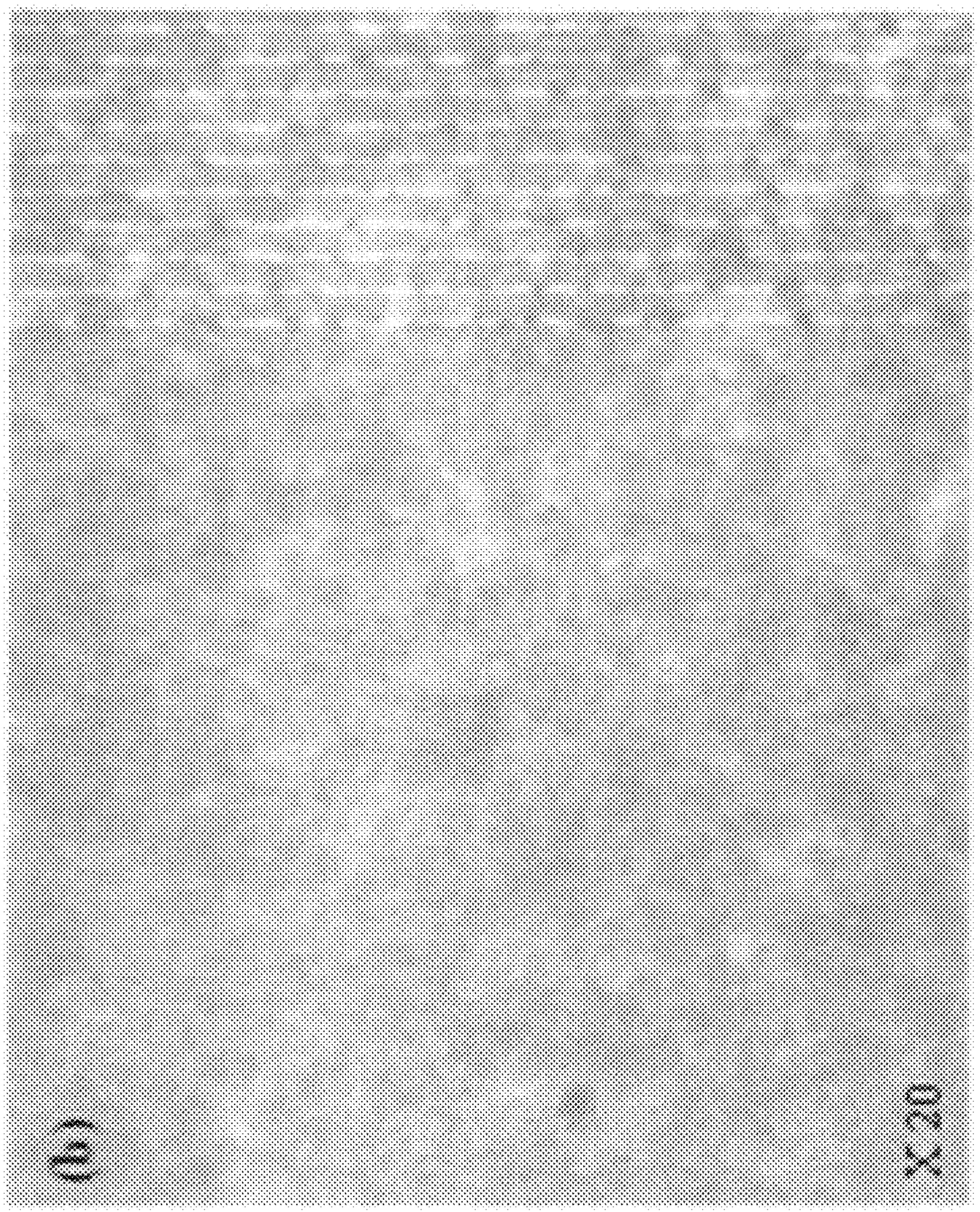

Fig. 24

After ultrasonication cleaning in acetone for 3 hours

Fig. 26

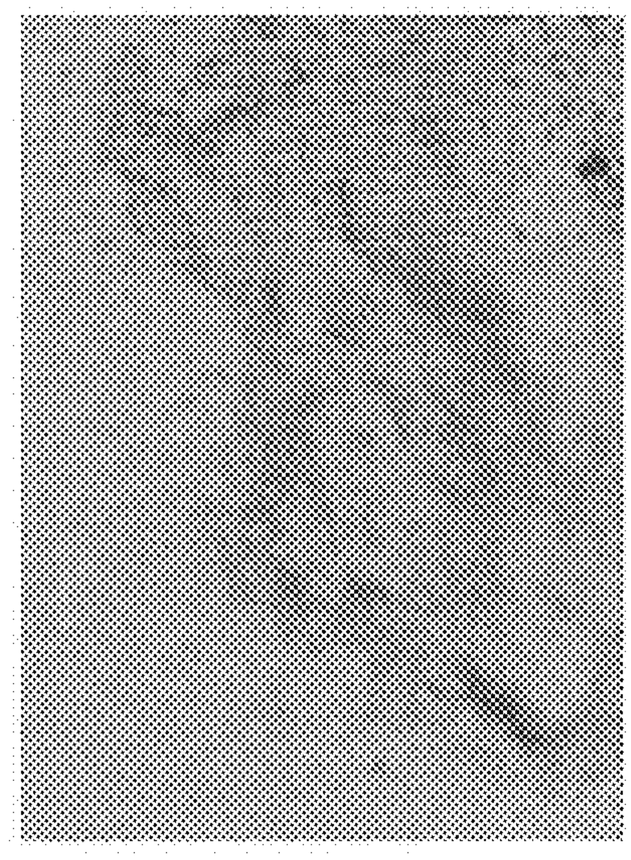

After DI water cleaning

Fig. 25

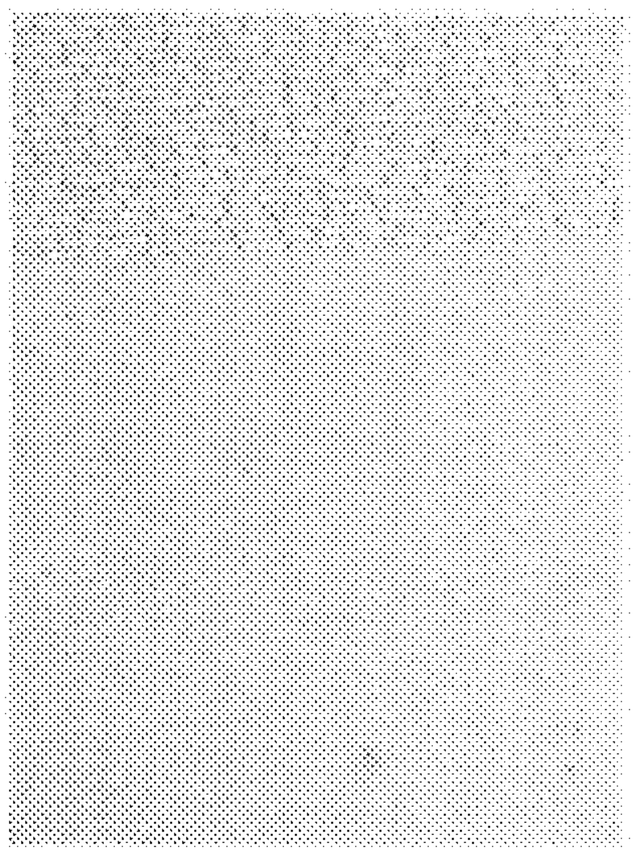

After 2nd biofilm growth experiment and oxygen plasma cleaning

Fig. 28

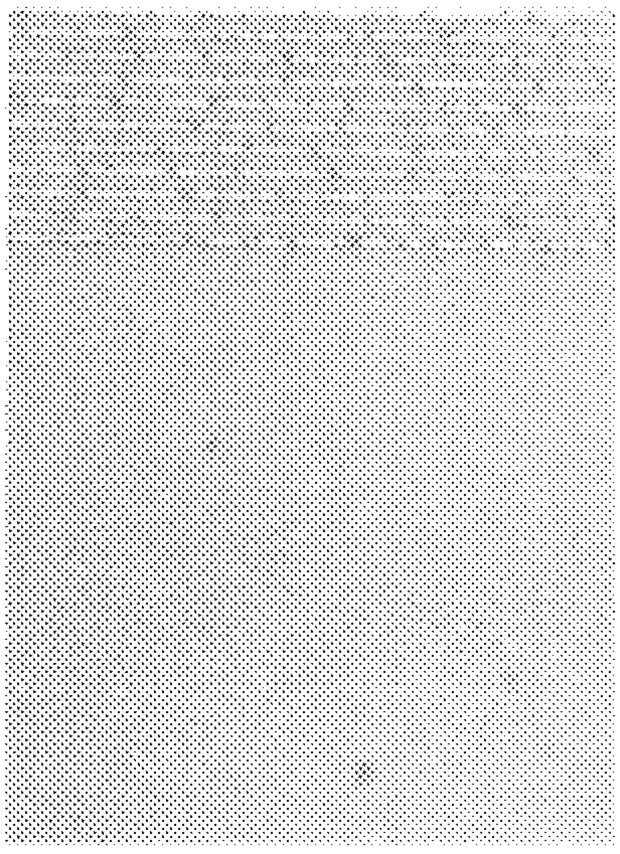

After oxygen plasma cleaning for 30s

Fig. 27

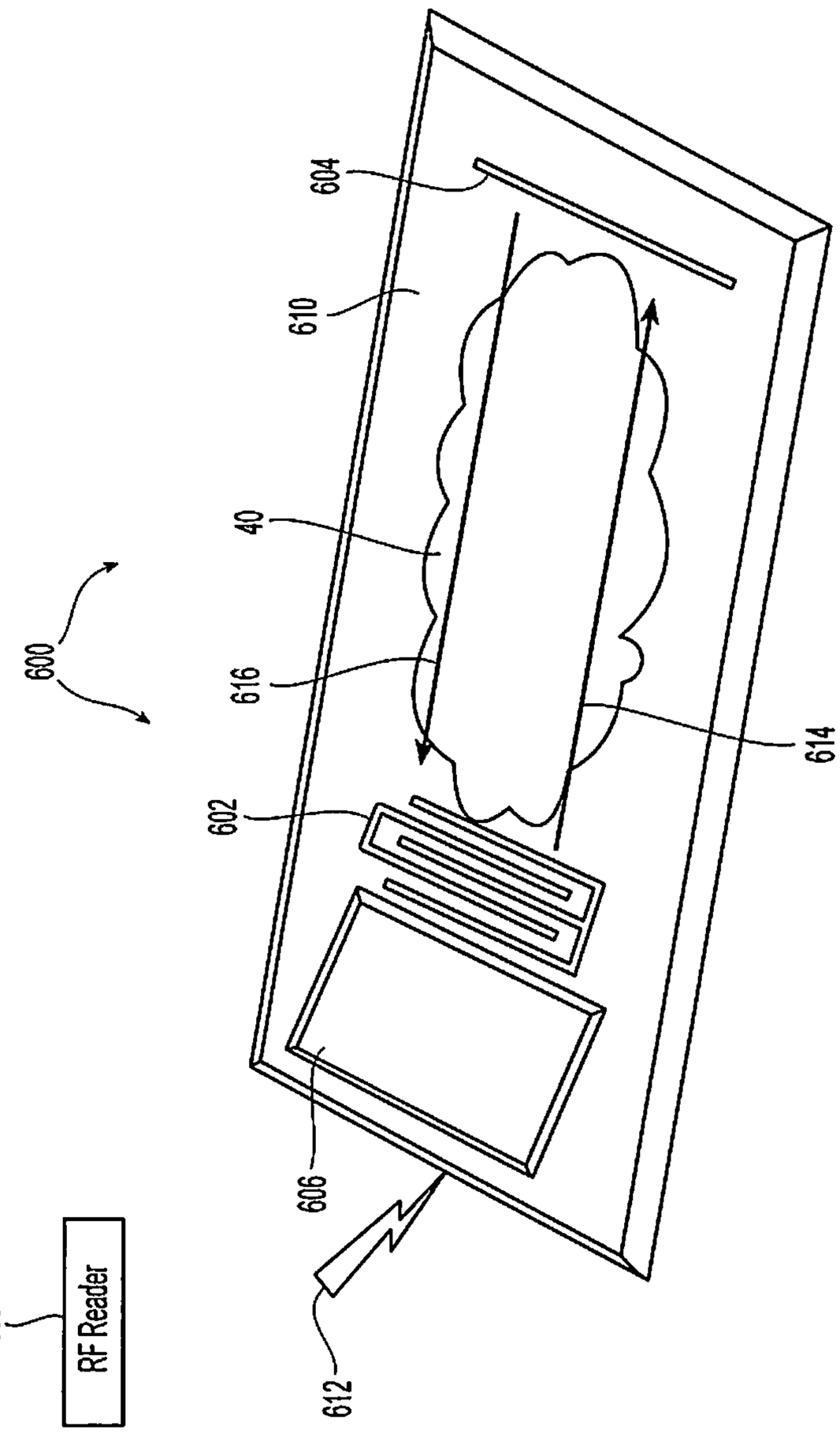

Fig. 29

ATOMIC LAYER DEPOSITION INVERTED PASSIVATED SURFACE ACOUSTIC WAVE SENSOR FOR EARLY DETECTION OF BIOFILM GROWTH

CROSS-REFERENCE TO RELATED APPLICATIONS

This application claims the benefit of, and priority to, U.S. Provisional Patent Application Ser. No. 61/753,332, filed on Jan. 16, 2013, entitled "ALD Passivated Bacterial Biofilm Sensor Using Inverted Surface. Acoustic Wave" by Young Wook Kim et al., the entire contents of which is hereby incorporated by reference herein.

STATEMENT OF GOVERNMENT SUPPORT

This invention was made with U.S. government support under EFRI1042881 awarded by the National Science Foundation. The U.S. government has certain rights in the invention.

BACKGROUND

1. Technical Field

The present disclosure relates to surface acoustic wave (SAW) sensors for detecting the growth of biofilms. More particularly, the present disclosure relates to piezoelectric SAW sensors having passivation film layer.

2. Background of Related Art

Bacteria can attach to surfaces and form microcolonies as their population increases. The colonies eventually can form a community known as a bacterial biofilm [1, 2]. A biofilm is not simply a group of bacteria, but a complex collection of microorganisms encased in an extracellular matrix. The extracellular matrix is composed of exopolysaccharide polymers which promote irreversible adhesion of microcolonies on the surface and also prevent diffusion of antibiotics through the biofilm [1, 2]. Due to the complex extracellular matrix and heterogeneous bacterial composition, biofilms are resistant to bacteriophages in industry and to chemically diverse antibiotic treatments in clinical fields [3]. In addition, bacterial corrosion of metals is an economically important consequence of bacterial biofilm formation that illustrates several fascinating aspects of the structure and physiology of these adherent bacterial populations. Therefore, environmental, clinical, and industrial long term reliable biofilm growth monitoring is critical to prevent contamination, severe infection, and corrosive problems due to the biofilm formation.

The measurement of bacterial biofilms with capacitive sensing has been applied by Yang and Li to monitor *Salmonella typhimurium* bacteria [4], and by Ghafar-Zadeh et al. to detect *Escherichia coil* (*E. coli*) [5]. In Yang and Li at al. [4], an interdigitated microelectrode was fabricated to provide detectable impedance signals in capacitance measurement during bacterial growth, *S. typhimurium* bacteria were grown over the microelectrode and the capacitance change was continuously measured. Capacitive sensing in a liquid environment, however, can be interfered with by a conductive media due to the current flow through the growth media [4].

The direct impedance measurement of the attachment of *E. coli* on an electrode is demonstrated by other groups [6, 7]. The change of impedance during bacterial growth is correlated with the biomass adhere on the electrode. This impedimetric sensing is particularly useful in detecting very early attachment of bacteria based on the significant impedance change observed upon attachment. However, long-term real-time biofilm monitoring by impedance measurement requires a continuous current source for bacterial detection which may cause interruption of bacterial growth.

Fluorescent methods have reported high sensitivity [8], but require fluorescent molecule labeling for sensing to occur. Labeling requires additional sample preparation and the fluorescent molecule can be degraded over long term exposure to liquid.

Electrochemical sensing can be used for selective detection a molecule without fluorescent labeling [9]. An electrochemical sensor array was integrated with a miniaturized bioreactor system for high throughput cell cultivation in 96 well plates [10]. Using a 100 μl working volume in the 96 well micro reactors, the sensor array can monitor temperature, pH, and oxygen concentration as well as total biomass. However, electrochemical sensors require a continuous power source for the operation and also require recalibration of the sensor due to the conductivity change of bacterial growth media in long term biofilm growth experiments.

Surface Acoustic Wave (SAW) sensors exhibit several advantages in small molecule detection including high sensitivity [11-22] and low power consumption [23]. A SAW sensor can detect mass or viscosity change due to the wave velocity attenuation, resulting in a resonant frequency shift at the output. A highly sensitive SAW sensor for detection of interleukin-6 (IL-6), which is one of key molecules in human immune system, was reported. In Krishnamoorthy et al. [19], a specific receptor for IL-6 was immobilized on the surface of the SAW sensor. Based on the resonant frequency shift due to the IL-6 binding, the detection limit of the SAW sensor was approximately 10^{-18} g (grams). A SAW sensor is also a passive device.

The power for operation of the SAW sensor can be delivered by an external device wirelessly which makes the SAW sensor useful for long term biofilm monitoring without a continuous power supply [23]. Furthermore, the SAW sensor can be fabricated using biocompatible materials [24-26]. The combination of extremely high sensitivity, biocompatibility, and low power consumption makes the SAW sensor a unique tool for real time monitoring of bacterial biofilm growth. However, it is also noted that piezoelectric materials used in the SAW sensor can be dissolved due to long term exposure to liquid [27].

SUMMARY

The present disclosure relates to a novel inverted passivated SAW sensor for real time biofilm monitoring. A piezoelectric film is deposited by pulsed laser deposition, and the sensor is effectively passivated by a passivated film layer using atomic layer deposition to prevent damage to the piezoelectric layer in bacterial growth media and animal serum.

The SAW sensor can be reused after oxygen plasma cleaning, allowing for consecutive biofilm formation experiments using one sensor.

Therefore, the present disclosure relates to a novel surface acoustic wave (SAW) biofilm sensor comprising: a SAW transducer; a piezoelectric film layer; and a passivation film layer. The piezoelectric film layer is mounted over the SAW transducer and the passivation film layer is mounted over the piezoelectric film layer. In one embodiment, the passivation layer includes aluminum oxide, Al_2O_3. In yet another embodiment, the passivation layer defines a thickness of at least 45 nanometers (nm). In a still further embodiment, the piezoelectric layer includes zinc oxide, ZnO. In yet another embodiment, the piezoelectric layer defines a thickness of at least 40 nanometers (nm).

The present disclosure relates also to a surface acoustic wave (SAW) biofilm sensor that includes a transmitting electric to acoustic wave transducer defining an upper surface and a lower surface, a receiving acoustic wave to electric transducer defining an upper surface and a lower surface, a piezoelectric film layer defining an upper surface and a lower surface and a passivation film layer defining an upper surface and a lower surface. A portion of the lower surface of the piezoelectric film layer is disposed on the upper surface of the transmitting electric to acoustic wave transducer and another portion of the lower surface of the piezoelectric film layer is disposed on the upper surface of the receiving acoustic wave to electric transducer and the lower surface of the passivation film layer is disposed on the upper surface of the piezoelectric film layer. The upper surface of the passivation film layer thereby configured to enable contact with a biofilm.

In one embodiment, the SAW biofilm sensor may further include a piezoelectric SAW loss reduction film layer defining an upper surface and a lower surface wherein the lower surface of the transmitting electric to acoustic wave transducer is disposed on a portion of the upper surface of the piezoelectric SAW loss reduction film layer and wherein the lower surface of the receiving acoustic wave to electric transducer is disposed on another portion of the upper surface of the piezoelectric SAW loss reduction film layer.

In still another embodiment, the SAW biofilm sensor may further include a substrate defining an upper surface and a lower surface, wherein the lower surface of the piezoelectric SAW loss reduction film layer is disposed on the upper surface of the substrate.

In yet another embodiment, a portion of the lower surface of the piezoelectric film layer is disposed on a portion of the upper surface of the piezoelectric SAW loss reduction film layer and disposed between the transmitting electric to acoustic wave transducer and the receiving acoustic wave to electric transducer.

In a still further embodiment, another portion of the lower surface of the piezoelectric film layer may be disposed between the transmitting electric to acoustic wave transducer and the receiving acoustic wave to electric transducer.

In one embodiment of the SAW biofilm sensor, wherein the piezoelectric layer defines an upper sub-layer and a lower sub-layer, wherein the lower sub-layer defined by the portion of the lower surface of the piezoelectric film layer is disposed on the portion of the upper surface of the lower piezoelectric film layer and is disposed between the transmitting electric to acoustic wave transducer and the receiving acoustic wave to electric transducer. The upper sub-layer is defined by the portion of the piezoelectric layer between the passivation film layer and the lower sub-layer. The lower sub-layer has a shear modulus and density to define a first SAW velocity. The upper sub-layer has a shear modulus and density to define a second SAW velocity wherein the second velocity differs from the first velocity.

In one embodiment, the second velocity is equal to or greater than the first velocity.

In still another embodiment, the SAW biofilm sensor the passivation layer includes aluminum oxide, Al_2O_3. In one embodiment, the passivation layer defines a thickness between the upper surface of the passivation layer and the lower surface of the passivation layer wherein the thickness of the passivation layer has a dimension of at least 45 nanometers (nm).

In yet another embodiment, the piezoelectric layer may include zinc oxide, ZnO. In one embodiment, the piezoelectric layer defines a thickness between the upper surface of the piezoelectric layer and the lower surface of the piezoelectric layer and the thickness of the piezoelectric layer has a dimension of at least 40 nanometers (nm).

The present disclosure relates also to a method of assembling a biofilm surface acoustic wave (SAW) sensor that includes depositing a piezoelectric layer on a SAW transducer electrode pattern and depositing a passivation layer on the piezoelectric layer.

In one embodiment, the depositing of the piezoelectric layer may include depositing a layer of zinc oxide ZnO on the SAW transducer electrode pattern. In a still further embodiment, the depositing a layer of zinc oxide ZnO on the SAW transducer electrode pattern may include depositing a layer of zinc oxide ZnO having a thickness of at least 40 nanometers (nm).

In yet another embodiment, the depositing a passivation layer on the piezoelectric layer may include depositing a layer of aluminum oxide Al_2O_3 on the piezoelectric layer.

In a still further embodiment, the depositing of the layer of aluminum oxide Al_2O_3 on the piezoelectric layer may include depositing a layer of aluminum oxide Al_2O_3 having a thickness of at least 45 nanometers (nm) on the piezoelectric layer.

In one embodiment, the method of assembling may further include depositing the SAW transducer electrode pattern on a piezoelectric SAW loss reduction film layer. The method may further include depositing the piezoelectric SAW loss reduction film layer on a substrate.

In another embodiment, the step of depositing the piezoelectric layer on the SAW transducer electrode pattern includes pulsed laser deposition.

In still another embodiment, the step of depositing the passivation layer on the piezoelectric layer includes atomic layer deposition.

BRIEF DESCRIPTION OF THE DRAWINGS

These and other advantages will become more apparent from the following detailed description of the various embodiments of the present disclosure with reference to the drawings wherein:

FIG. **1** illustrates a cross-sectional view of an example of a coated piezoelectric SAW transducer according to the prior art:

FIG. **2** illustrates a top perspective view of an exemplary embodiment of an uncoated piezoelectric SAW transducer within a piezoelectric substrate that is utilized to receive a passivation film according to one embodiment of the present disclosure;

FIG. **3** illustrates a cross-sectional view of a coated piezoelectric SAW transducer biofilm sensor according to one embodiment of the present disclosure:

FIG. **4**A illustrates a top perspective schematic view of an exemplary embodiment of the SAW biofilm sensor of FIGS. **2** and **3** according to one embodiment of the present disclosure that includes the piezoelectric SAW transducer of FIG. **2** further including a piezoelectric layer and a passivation layer disposed on the upper surface of the SAW transducer and further illustrating a SAW passing through a biofilm on the upper surface of the passivation layer;

FIG. **4**B illustrates a cross-sectional schematic view of the SAW biofilm sensor of FIG. **4**A illustrating the piezoelectric transducer and the thickness dimensions of the piezoelectric layer, the passivation layer and the biofilm;

FIG. **5** illustrates a schematic diagram of pulsed layer deposition of the piezoelectric layer on a substrate for assembling the piezoelectric SAW biofilm sensor of FIGS. **2**, **3**, **4**A and **4**B;

FIG. **6** illustrates a schematic diagram of atomic layer deposition of the passivation layer of FIGS. **3**, **4**A and **4**B;

FIG. **7**A is a schematic illustration of a piezoelectric SAW loss reduction film layer deposited on a substrate;

FIG. **7**B is a schematic diagram of an interdigitated piezoelectric SAW transducer electrode pattern deposited on the piezoelectric SAW loss reduction film layer of FIG. **7**A;

FIG. **7**C is a schematic diagram of a piezoelectric layer deposited on the electrode pattern and the piezoelectric SAW loss reduction film layer deposited on a substrate of FIGS. **7**A and **7**B;

FIG. **7**D is a schematic diagram of the piezoelectric layer and electrode pattern of FIG. **7**C undergoing annealing;

FIG. **7**E is a schematic diagram of a passivation layer deposited partially on the electrode pattern of FIGS. **7**B, **7**C and **7**D and on the piezoelectric layer of FIGS. **7**C and **7**D;

FIG. **8** is a graphical plot of normalized sensitivity of a SAW biofilm sensor assembled in accordance with FIGS. **2**-**7**E for various passivation layer materials including without passivation;

FIG. **9** is an optical microscopy image of a SAW biofilm sensor assembled in accordance with FIGS. **2**-**7**E passivated by ALD of Al_2O_3 with a passivation layer thickness of 20 nanometers (nm) showing damaged areas;

FIG. **10** is an optical microscopy image of another SAW biofilm sensor assembled in accordance with FIGS. **2**-**7**E passivated by ALD of Al_2O_3 with a passivation layer thickness of 30 nm showing damaged areas;

FIG. **11** is an optical microscopy image of yet another SAW biofilm sensor assembled in accordance with FIGS. **2**-**7**E passivated by ALD of Al_2O_3 with a passivation layer thickness of 40 nm showing damaged areas;

FIG. **12** is an optical microscopy image of another SAW biofilm sensor assembled in accordance with FIGS. **2**-**7**E passivated by ALD of Al_2O_3 with a passivation layer thickness of 45 nm showing no damage;

FIG. **13** is an optical surface image of another SAW biofilm sensor assembled in accordance with FIGS. **2**-**7**E passivated by a 45 nm Al_2O_3 film using e-beam evaporation showing damage;

FIG. **14** is an optical surface image of another SAW biofilm sensor assembled in accordance with FIGS. **2**-**7**E passivated by a 45 nm Al_2O_3 film using RF sputtering showing damage;

FIG. **15** is an optical surface image of another SAW biofilm sensor assembled in accordance with FIGS. **2**-**7**E passivated by a 45 nm Al_2O_3 film using ALD showing no damage;

FIG. **16** is a top perspective view of a SAW biofilm sensor assembled in accordance with FIGS. **2**-**7**E as a packaged unit together with other components for biofilm sensing according to one embodiment of the present disclosure;

FIG. **17** is an optical microscopy image of the surface of a SAW biofilm sensor assembled in accordance with FIGS. **2**-**7**E before biofilm cleaning;

FIG. **18** is an optical microscopy image of the surface of the SAW biofilm sensor assembled in accordance with FIGS. **2**-**7**E after oxygen plasma biofilm cleaning;

FIG. **19** is a graphical plot of negative resonant frequency shift results for SAW biofilm sensors assembled in accordance with FIGS. **2**-**7**E versus time due to lysogeny broth (LB) biofilm growth for three newly fabricated SAW transducers;

FIG. **20** is a graphical plot of negative resonant frequency shift results for a SAW biofilm sensor assembled in accordance with FIGS. **2**-**7**E versus time due to lysogeny broth biofilm growth in three sequential growth experiments using one device in an LB;

FIG. **21** is a graphical plot of negative resonant frequency shift results for a SAW biofilm sensor assembled in accordance with FIGS. **2**-**7**E versus time in three growth experiments using a newly fabricated sensor in 10% fetal bovine serum (FBS);

FIG. **22** is a graphical plot of averaged biofilm thickness and standard deviation in LB media and in 10% FBS over 30-40 locations measured by optical microscopy;

FIG. **23** is a microscopy image of a SAW biofilm sensor assembled in accordance with FIGS. **2**-**7**E after biofilm growth experiments in LB media;

FIG. **24** is a microscopy image of the SAW biofilm sensor of FIG. **23** assembled in accordance with FIGS. **2**-**7**E after biofilm growth experiments in 10% FBS;

FIG. **25** is a microscopy image of a SAW biofilm sensor assembled in accordance with FIGS. **2**-**7**E after cleaning with deionized water;

FIG. **26** is a microscopy image of the SAW biofilm sensor of RIG, 25 after ultrasonication cleaning in acetone for 3 hours;

FIG. **27** is a microscopy image of the SAW biofilm sensor of FIGS. **25** and **26** after oxygen plasma cleaning for 30 seconds;

FIG. **28** is a microscopy image of the SAW biofilm sensor of FIGS. **25**, **26** and **27** after a second biofilm growth experiment and oxygen plasma cleaning for 30 seconds; and

FIG. **29** is a perspective view a top perspective view of an exemplary embodiment of a SAW biofilm sensor that includes an antenna for radiofrequency (RF) coupling to a radiofrequency identification (RFID) reader.

DETAILED DESCRIPTION

The present disclosure relates to the design of a passivated piezoelectric SAW transducer biofilm sensor according to embodiments of the present disclosure without loss of sensitivity for biosensing applications.

First, to illustrate the advantages of the embodiments of the present disclosure, FIG. **1** illustrates an example of a prior art SAW biofilm sensor **10** wherein the piezoelectric materials used in the SAW biofilm sensor can be dissolved due to long term exposure to liquid. More particularly, SAW biofilm sensor **10** includes a SAW transducer **20** having a transmitting electrode transducer **22** and a receiving electrode transducer **24** each mounted over a common piezoelectric loss reduction film **30** and a substrate **32**. The common piezoelectric loss reduction film **30** and substrate **32** form a transducer mounting structure **35**. The transmitting electrode transducer **22** includes an elevated portion **23** and the receiving electrode transducer **24** includes a corresponding interfacing elevated portion **25** which are each raised above upper surface **30***a* of the common piezoelectric loss reduction film **30**. Both the elevated portion **23** and the elevated portion **25** are elevated above, and not in contact with, the upper surface **30***a* to provide a space above the common piezoelectric loss reduction film **30** for a thin film **26** in contact with, and mounted over, the common piezoelectric loss reduction film **30**. The elevated portions **23** and **25** each extend partially over upper surface **26***a* of the thin film **26**. During usage, a biofilm **40** is positioned over both the elevated portions **23** and **25** and upper surface **26***a* of the thin film **26**.

The substrate **32** may be made from silicon Si and the common piezoelectric loss reduction film **30** may be made from silicon dioxide SiO_2.

Since the biofilm **40** is in direct contact with the elevated portions **23** and **25** of the transmitting electrode transducer **22** and the receiving electrode transducer **24**, respectively, the

configuration of a SAW sensor such as SAW sensor **10** in FIG. **1** has been shown to be susceptible to dissolution of the common piezoelectric film **30** due to long term exposure to the liquid biofilm.

In contrast, the present disclosure relates to a successfully passivated ZnO based SAW sensor for long term biofilm growth monitoring in an animal serum or bacterial growth media. Atomic Layer Deposition (ALD) was applied for high density and conformal aluminum oxide (Al_2O_3) film deposition to protect the ZnO of the SAW sensor from media. The SAW sensor was used for the in vitro real time study of *E. coli* static biofilm growth in Lysogeny Broth (LB) media and in 10% Fetal Bovine Serum (FBS), the latter of which is the most widely used serum for mammalian cell culture due to similarities to in vivo environments [28].

The remainder of the present disclosure presents the design of the inverted SAW sensor for the targeted mode of the wave and fabrication process. The material and experimental procedures for biofilm detection in the sensor are presented. The results show the biofilm detection using the sensor in consecutive testing both in bacterial growth media and animal serum.

More particularly, FIG. **2** illustrates a top perspective view of an exemplary embodiment of an uncoated piezoelectric SAW transducer **100** having a transmitting electric to acoustic wave transducer **110** and a receiving acoustic wave to electric transducer **110'** both mounted on upper surface **30***a* of the transducer mounting substrate **35** of FIG. **1** that is utilized to receive a passivation film according to one embodiment of the present disclosure. The transmitting electric to acoustic wave transducer **110** and the receiving acoustic wave to electric transducer **110'** together define an interdigitated SAW transducer **105** as is known in the art. The transmitting electric to acoustic wave transducer **110** includes a first transmitting electrode comb-like or prong-like electrically conductive member **112** that interlocks or interdigitates with a second transmitting electrode comb-like electrically conductive member **122**. The first transmitting conductive member **112** includes a rectangularly-shaped base **114** from which extend orthogonally first rectangularly-shaped peripheral prong **116***a*, rectangularly-shaped central prong **116***b* and second rectangularly-shaped peripheral prong **116***c*.

As noted, the transmitting electric to acoustic wave transducer **110** also includes the second transmitting electrode comb-like or prong-like electrically conductive member **122** that interlocks or interdigitated with the first transmitting electrode comb-like electrically conductive member **112**. The second transmitting conductive member **122** includes a rectangularly-shaped base **124** from which extend orthogonally first rectangularly-shaped prong **126***a* and second rectangularly-shaped prong **126***b*. The rectangularly shaped base **124** defines a first end **124***a* and a second end **124***h*. The first prong **126***a* is positioned at a distance away from first end **124***a* and the second prong **1261** is positioned at a distance away from the second end **126***b* to define a central rectangularly-shaped aperture **128** between the first prong **126***a* and the second prong **126***b*.

The first transmitting electrically conductive member **112** includes a voltage input terminal Vin that is in direct electrical communication with, for example, the rectangularly-shaped base **114** such that the entire first transmitting electrically conductive member **112** is in electrical communication with the voltage input terminal Vin. The first and second electrically conductive members **112** and **122** are arranged such that the prongs **116***a*, **116***b*, **116***c* are adjacent to and intermesh with prongs **126***a* and **126***h*. The second transmitting electrically conductive member **122** includes a ground terminal **130** that is in direct electrical communication with, for example, the rectangularly-shaped base **124** such that the entire second transmitting electrically conductive member **122** is in electrical communication with the ground terminal **130**.

The receiving acoustic wave to electric transducer **110'** includes the same components as, and is arranged in the same manner as, transmitting electric to acoustic wave transducer **110** and for convenience the components are designated with primes.

Consequently, receiving acoustic wave to electric transducer **110'** includes a first transmitting electrode comb-like or prong-like electrically conductive member **112'** that interlocks or interdigitates with a second transmitting electrode comb-like electrically conductive member **122'**. The first receiving electrically conductive member **112'** includes rectangularly-shaped base **114** from which extend orthogonally first rectangularly-shaped peripheral prong **116***a'*, rectangularly-shaped central prong **116***b'* and second rectangularly-shaped peripheral prong **116***c'*.

The receiving electric to acoustic wave transducer **110'** also includes the second receiving electrode comb-like or prong-like electrically conductive member **122'** that interlocks or interdigitates with the first receiving electrode comb-like electrically conductive member **112'**. The second receiving conductive member **122'** includes a rectangularly-shaped base **124'** from which extend orthogonally first rectangularly-shaped prong **126***a'* and second rectangularly-shaped prong **126***b'*. The rectangularly-shaped base **124'** defines a first end **124***a'* and a second end **124***b'*. The first prong **126***a'* is positioned at a distance away from first end **124***a'* and the second prong **126***b'* is positioned at a distance away from the second end **126***b'* to define a central rectangularly-shaped aperture **128'** between the first prong **126***a'* and the second prong **126***b'*.

The first receiving electrically conductive member **112'** includes a voltage output terminal Vout that is in direct electrical communication with, for example, the rectangularly-shaped base **114'** such that the entire first receiving electrically conductive member **112'** is in electrical communication with the voltage output terminal Vout. The first and second electrically conductive members **112'** and **122'** are arranged such that the prongs **116***a'*, **116***b'*, **116***c'* are adjacent to and intermesh with prongs **126***a'* and **126***h'*. The second receiving electrically conductive member **122'** includes a ground terminal **130'** that is in direct electrical communication with, for example, the rectangularly-shaped base **124'** such that the entire second receiving electrically conductive member **122'** is in electrical communication with the ground terminal **130'**.

When a voltage source, not shown, is placed across the terminals Vin and Vout, a surface acoustic wave **150** is generated by the transmitting electric to acoustic wave transducer **110** and travels in the direction of arrow **152** towards the receiving acoustic wave to electric transducer **110'**.

FIG. **3** illustrates a cross-sectional view of a coated piezoelectric SAW transducer biofilm sensor **200** according to one embodiment of the present disclosure. More particularly, surface acoustic wave (SAW) biofilm sensor **200** includes the interdigitated SAW transducer **105** of FIG. **2**. Accordingly, the SAW biofilm sensor **200** includes transmitting electric to acoustic wave transducer **110** defining an upper surface **110***a* and a lower surface **110***b* where the cross-section (not shown) is taken through the rectangularly-shaped base **124**. The surface acoustic wave (SAW) biofilm sensor **200** also includes receiving acoustic wave to electric transducer **110'** defining an upper surface **110***a'* and a lower surface **110***b'*.

The lower surface **110***a* of the transmitting electric to acoustic wave transducer **110** is disposed on a portion **301***a* of

the upper surface **30***a* of the piezoelectric SAW loss reduction film layer **30** and the lower surface **110***a*' of the receiving acoustic wave to electric transducer **110**' is disposed on another portion **302***a* of the upper surface **30***a* of the piezoelectric SAW loss reduction film layer **30**.

A piezoelectric film layer **160** defines an upper surface **160***a* and a lower surface **160***b*. A portion **1601***b* of the lower surface **160***b* of the piezoelectric film layer **160** is disposed on the upper surface **110***a* of the transmitting electric to acoustic wave transducer **110**. Another portion **1602***b* of the lower surface **160***b* of the piezoelectric film layer **160** is disposed on the upper surface **110**'*a* of the receiving acoustic wave to electric transducer **110**'.

A passivation film layer **170** defines an upper surface **170***a* and a lower surface **170***b*, The lower surface **170***b* of the passivation film layer **170** is disposed on the upper surface **160***a* of the piezoelectric film layer **160**. Thus, the upper surface **160***a* of the passivation film layer **170** is thereby configured to enable contact with a biofilm **40**.

In a similar manner as described with respect to FIG. **1**, the coated piezoelectric SAW transducer biofilm sensor **200** may be disposed or mounted on transducer mounting structure **35** which include common piezoelectric loss reduction film layer **30** and substrate **32**. The substrate **32** defines an upper surface **32***a* and a lower surface **32***b*. Similarly, the common piezoelectric loss reduction film layer **30** defines the upper surface **30***a* and a lower surface **30***b*. The lower surface **30***b* of the piezoelectric SAW loss reduction film layer **3030** is disposed on the upper surface **32***a* of the substrate **32**.

A portion **1603***b* of the lower surface **160***b* of the piezoelectric film layer **160** is disposed on a portion **303***a* of the upper surface **30***a* of the piezoelectric SAW loss reduction film layer **30** and disposed between the transmitting electric to acoustic wave transducer **110** and the receiving acoustic wave to electric transducer **110**'.

FIG. **4**A illustrates a top perspective schematic view of the exemplary embodiment of the SAW biofilm sensor **200** of FIGS. **2** and **3** according to one embodiment of the present disclosure that includes the piezoelectric SAW transducer **105** further including the piezoelectric layer **160** and the passivation layer **170** disposed on the upper surfaces **110***a* and **110***a*' of the SAW transducer **105** and further illustrating a SAW **150** passing in the direction of arrow **152** through a biofilm **40** on the upper surface **170***a* of the passivation layer **170**.

FIG. **4**B illustrates a cross-sectional schematic view of the SAW biofilm sensor **200** of FIG. **4**A illustrating the piezoelectric transducer **105** and the thickness dimensions of the piezoelectric layer **160**, the passivation layer **170** and the biofilm **40**. More particularly, in the exemplary embodiment of FIG. **4**B, the piezoelectric layer **160** may define an upper sub-layer **162** and a lower sub-layer **161** which together define thickness d of the piezoelectric layer **160**.

The lower sub-layer **161** is defined by the portion **1603***b* of the lower surface **160***b* of the piezoelectric film layer **160** that is disposed on the portion **303***a* of the upper surface **30***a* of the lower piezoelectric film layer **30** and is disposed between the transmitting electric to acoustic wave transducer **110** and the receiving acoustic wave to electric transducer **110**'. The upper sub-layer **162** is defined by the portion of the piezoelectric layer **160** between the passivation film layer **170** and the lower sub-layer **161** of the piezoelectric layer.

The lower sub-layer **161** has a shear modulus and density to define a first SAW velocity V1. The upper sub-layer **162** has a shear modulus and density to define a second SAW velocity V2. Although the second velocity V2 may differ from the first velocity V1, for the purposes of simplifying the design analysis, the two velocities may be set equal to one another. Alternatively, the second velocity V2 may be equal to or greater than the first velocity V1.

The passivation layer **170** defines a thickness h between the upper surface **160***a* of the passivation layer **160** and the lower surface **160***b* of the passivation layer **160** while the biofilm **40** defines a thickness x.

In one embodiment, the piezoelectric layer **160** includes zinc oxide, ZnO and the thickness d of the piezoelectric layer **160** has a dimension of at least 40 nanometers (nm).

In one embodiment, the passivation layer includes aluminum oxide, Al_2O_3, and the thickness h of the passivation layer **170** has a dimension of at least 45 nanometers (nm).

The specific design for the selection of the material and thickness of the piezoelectric layer **160** and the passivation layer **170** is described in more detail below.

Materials and Methods

Design of the SAW Sensor

For applications of a SAW sensor in liquid environments, selecting the proper mode of propagation is crucial to prevent severe attenuation or the wave. In a SAW sensor, the surface of the piezoelectric layers is set to a high frequency oscillation governed by the design of the interdigitated transducers (IDT) and the SAW velocity of the piezoelectric material. This no-load oscillation frequency is affected by environmental changes at the surface of the SAW sensor. These effects are observed experimentally as changes in resonant frequency, representing a shift in the SAW phase velocity. However, one of the challenges for biosensor applications is the extremely high attenuation damping of the SAW in liquid environments, when Rayleigh mode waves are generated. In this mode the acoustic wave displacement is perpendicular to the surface and causes significant attenuation of the oscillations in liquid environments. Unlike Rayleigh mode waves, Love mode SAW generation demonstrates displacement planar to the surface and the oscillations are not attenuated in liquid environments [11-15, 18-20, 29-31]. The generation of Love or Rayleigh mode waves depends on the crystallographic orientation of the piezoelectric film. Therefore, it is highly advantageous to deposit piezoelectric material with a specific orientation for generating Love mode SAW [16-22, 29-31]. ZnO with a high piezoelectric coefficient is capable of generating very high frequency (GHz, gigahertz, where Hz is hertz or 1 cycle/sec) SAW, and it has been shown to grow along the crystallographic orientation that favors Love mode propagation on a SiO_2/Si substrate [19-22]. Love mode waves are predominantly generated with the SAW IDT aligned perpendicular to the c-axis of the ZnO film [16-22].

Some important parameters, such as the SiO.sub.2 thickness, the IDT electrode dimensions, and the ZnO deposition method, had to be considered in the design of a highly sensitive SAW sensor. In order to confine the propagation of the SAW on the surface of the device, a thin film that can prevent acoustic wave loss from the piezoelectric material to Si substrate was required between ZnO film and Si. SiO_2 was previously shown [15, 18] to be an appropriate loss blocking film for thicknesses around 50 nm and was selected in this work. For the best resonance of the SAW at the designed operational frequency, the IDT separation d should be equal to half of the operational wavelength λ. (See FIG. **7**B). The acoustic wave velocity for the ZnO thin film used in this work was 4814 m/s, and the operational frequency (401 MHz-406 MHz) of the SAW sensor was designed to meet the regulation set by the Federal Communication Commission (FCC) for future biomedical biofilm detection applications [32, 48]. This wavelength (λ) was 12 μm, rendering the electrode separation of the IDT 6 μm (λ/2). The crystal quality of ZnO film also had

to be high for a sensitive SAW sensor. The ZnO film with low impurities and lattice defects was achieved by PLD which has been widely used in metal oxides for high quality film deposition due to stoichiometric deposition with the target material [33] and a relatively simple set-up.

To achieve advantages over prior art biofilm sensors for biofilm detection, it was necessary to provide an inverted structure for the saw sensor **200**, as shown in FIGS. **3**, **4**A and **4**B as compared to the structure of a standard SAW sensor such as biofilm sensor **20** as shown in FIG. **1**. In traditional SAW sensors such as biofilm sensor **20**, the IDT is exposed to the liquid environment directly, causing IDT corrosion in long term studies. However, in the inverted SAW sensor **200** according to FIGS. **3**, **4**A and **4**B, the IDT lifetime is extended because the IDT is patterned under the piezoelectric film. The sensitivity of the Love mode SAW sensor in the top and bottom of piezoelectric films also show the same level of sensitivity for our designed ZnO film thickness (400 nm) based on the Love mode propagation depth [11-14, 29].

The material of the IDT, traditionally aluminum in the SAW sensor, can be selected by the acoustic impedance match theory [34]. Potential materials, such as aluminum and gold, were selected and the acoustic power reflective coefficient (R) was calculated based on the theory. The reflective coefficient of the aluminum and gold were 0.058 and 0.012 respectively. The lower reflective coefficient in IDT represents more energy transmission to the piezoelectric material which makes a highly sensitive SAW sensor. Therefore, the IDT material was chosen to be gold based on the low R value.

Selection of Passivation Film

Since the bare ZnO layer **160** without a passivation film layer **170** was damaged both in LB media and 10% FBS, selection of the proper material to protect ZnO while considering future biomedical applications is important to maintain the sensitivity of the sensor. The sensitivity of the passivated SAW sensor is decreased as compared to the unpassivated sensor due to the initial mass loading and dispersion of the wave in the passivation film [12, 29, 35-40]. To investigate the effect of the added material on the SAW sensitivity in addition to the material selection, we consider only the mass loading effect of the passivation film based on the assumption that the dispersion in the passivation film is minimal due to a much thinner passivation layer (45 nm) as compared to the wavelength of the SAW [35, 38, 40]. As noted, the schematic cross section view of the inverted passivation SAW sensor **200** is shown in FIGS. **3**, **4**A and **4**B. The sensitivity of the SAW sensor (S_m^v) is directly proportional to the velocity change due to the mass loading as shown in equation (1) [15, 18-20].

$$S_m^v = \lim_{\Delta m \to 0} \frac{1}{\Delta m}\left(\frac{\Delta v}{v_0}\right) \tag{1}$$

where v_0 is the initial velocity of the wave, m is the amount of the additional mass, and Δv is the wave velocity changes due to Δm. The SAW velocity (v), shown in equation (2), is defined by the shear modulus of the piezoelectric material and local area density based on the one-dimensional acoustic wave equation (3) [15, 18-20].

$$v = \sqrt{\frac{C}{p}} \tag{2}$$

-continued

$$\frac{\partial^2 u}{\partial t^2} = \left(\frac{C}{\rho}\right)\frac{\partial^2 u}{\partial y^2} \tag{3}$$

where C is the shear modulus of the surface material, u is the mechanical displacement of the piezoelectric substrate, ρ is material density of the surface, y is the axis of the mechanical displacement propagation, and v is the velocity of the SAW in equations (2) and (3). In order to simplify the modeling of passivation effects on the sensitivity of the SAW sensor, the bacterial growth over the sensor was assumed uniform, so that bacterial mass loading only depended on the thickness of the biofilm. Based on this assumption, the sensitivity of the SAW sensor from equation (1) was proportional to the velocity change as biofilm thickness (x) approaches zero as shown in equation (4).

$$S_m^v \propto \frac{dv}{dx_{x\to 0}} \tag{4}$$

The biofilm formed on the sensor also has a comparatively low shear modulus that can be neglected in the calculation of the total shear modulus of the passivated SAW sensor. The total shear modulus including the ZnO and the passivation film was calculated based on a mechanical spring series connection because the SAW is transferred from ZnO film to the passivation layer sequentially. Based on the assumptions and the total shear modulus calculation, the SAW velocity on a sensor coated with a biofilm was determined by the following equation (5).

$$v = \sqrt{\frac{C_{ZnO}}{\rho_{ZnO} d}\left(\frac{C_{film}}{C_{ZnO} + C_{film}}\right)\left(\frac{1}{1 + \frac{\rho_{film} h}{\rho_{ZnO} d} + \frac{\rho_{bac} x}{\rho_{ZnO}}}\right)} \tag{5}$$

where C_{film} and C_{Zno} are the shear moduli of the passivation film and ZnO, ρ_{Zno} and ρ_{film} are the densities of the ZnO and passivation film, h is the thickness of the passivation film, d is the thickness of the ZnO film, and x is the biofilm thickness. All parameters except the biofilm thickness (x) were determined by selecting potential passivation materials (i.e. Al_2O_3, Si_3N_4, SiO_2 and Teflon) and their thicknesses which were assumed to be 40 nm for all passivation films considered. Potential passivation materials with mechanical properties similar to the ZnO film, such as shear modulus and density, were selected [41, 42]. The sensitivity of the SAW sensor with different passivation films was calculated by differentiating equation (5) with respect to x, and letting x approach zero, based on equation (4).

FIG. **8** graphically illustrates the normalized theoretical sensitivity for, from left to right, without passivation, aluminum oxide —Al_2O_3, silicon nitride —Si_3N_4, silicon dioxide —SiO_2, and Teflon. The lowest degradation in sensitivity is observed for the Al_2O_3 passivation layer with a 0.20 reduction, while Teflon had the maximum degradation at 0.95 reduction.

The application of this fundamental theoretical treatment showed that an Al_2O_3 film was best suited as a passivation layer and it was selected. The thickness of the passivation film (h) in equation (5) is important for our application. The film should be thick enough for effective passivation, but should not be too thick that the added layer causes a significant

attenuation both due to mass loading and dispersion of the SAW resulting in substantial loss in sensitivity. The minimum required thickness of Al_2O_1 film (45 nm) was empirically determined. The detailed studies were presented in the film characterization section.

Fabrication

As described below in more detail with respect to FIG. **5**, to create the piezoelectric layer **160** on the transducer mounting structure **35**, the target material employed herein is zinc oxide, ZnO. Stoichiometric film deposition is achieved by application of a 248 nm KrF laser in 25 ns pulses at 250° C.

FIG. **6** illustrates a schematic diagram of atomic layer deposition of the passivation layer **170** of FIGS. **3**, **4**A and **4**B.

The fabrication process flow is shown in FIGS. **7**A through **7**E. Referring first to FIG. **7**A, a silicon dioxide (SiO_2) layer **30** was deposited on the upper surfaces **32***a* of (100) Si substrates **32** by low pressure chemical vapor deposition (LPCVD) as studied in [15, 22].

Referring to FIG. **7**B, the IDT **105** was patterned using traditional photolithography before depositing the piezoelectric layer **160**, e.g., ZnO film. The IDT prongs **116***a* and **116***a*' are deposited to have a width W1 of 1 μm (microns), prongs **116***b* and **116***b*' are deposited to have a width W2 of 1.5 μm, and prongs **116***c* and **116***c*' are deposited to have a width W3 of 2 μm. Due to the small feature size of the IDT **105**, including 1 μm, 1.5 μm, and 2 μm wide electrodes, oxygen plasma was used to remove residual photoresist after development.

In FIG. **7**C, Cr/Au (15 nm/200 nm) as the IDT **105** material was deposited on the wafer or transducer mounting structure **35** by E-beam evaporation, followed by lift-off. The transducer mounting structure **35** was diced into smaller segments before deposition of the piezoelectric layer **160**, composed of ZnO, was performed by pulsed laser deposition (PLD). Crystalline [001] orientation ZnO films on SiO_2/(100)Si substrates were grown by PLD. The piezoelectric layer **160** did not entirely cover the IDT **105** such that an indentation **162***a* from longitudinal external edge **1161***a* of the prong **116***a* and an indentation **162***b* from longitudinal external edge **1162***c*' of the prong **116***c*' were formed in the piezoelectric layer **160** to subsequently accommodate portions of the passivation layer **170**.

FIG. **7**D illustrates the annealing process of the ZnO film pattern wherein the ZnO film pattern was annealed at 800° C. for 1 hour.

FIG. **7**E is a schematic diagram of passivation layer **170** deposited partially on the electrode pattern **105** of FIGS. **7**B, **7**C and **7**D and on the piezoelectric layer **160** of FIGS. **7**C and **7**D. Vertical edges **172***a*, **172***b* of the passivation layer **170** are formed by the atomic layer deposition to fill the indentations **162***a*, **162***b*, respectively, of the piezoelectric layer **160**.

For simplicity, in FIGS. **7**B to **7**E, only the prongs **116***a*, **116***b*, **116***c* of the first transmitting electrically conductive member **112** and only the prongs **116***a*', **116***b*', **116***c*' of the first receiving electrically conductive member **112**' as shown in FIG. **2** are illustrated. The second transmitting electrically conductive member **122** and the second receiving electrically conductive member **122**' are omitted in FIGS. **7**B to **7**E.

Returning to FIG. **5**, there is illustrated a schematic diagram of a pulsed layer deposition (PLD) system for the piezoelectric layer **160** on the transducer mounting structure **35** that includes common piezoelectric loss reduction layer **30** and substrate **32** for assembling the piezoelectric SAW biofilm sensor **200** of FIGS. **2**, **3**, **4**A and **4**B. More particularly, pulsed laser deposition (PLD) system **300** includes a vacuum chamber **302** having a rotating target carousel **304**. The carousel is rotatable by a first shaft **306** which passes through a first penetration **308** in the vacuum chamber **302**. The shaft **306** rotates a platform **310** supported on the target carousel **304** and supports the target **312** which is thus capable of being rotated by the first shaft **306**.

The transducer mounting structure **35** is positioned directly opposite to the target **312** on the target platform **310** and the target carousel **304**. The structure **35** is positioned on a heatable sample stage **314** that is supported by a second shaft **316** that passes through a second penetration **318** in the vacuum chamber **302**.

A quartz window **320** is positioned in the vacuum chamber **302** at an angle to enable a beam of laser light **324** to impact the target **312**. As a result of the beam of laser light **324** impacting the target **312**, a plume **326** of target material is created within the vacuum chamber and deposits on the transducer mounting structure **35** which includes substrate **32**.

The laser deposition system used a KrF excimer laser at a wavelength of 248 nm with pulse duration of 25 ns to ablate a high purity (99.99%) ZnO ceramic target. The ZnO layer was grown at 250° C. with an ambient oxygen partial pressure of ~1.0×10^{-4} Torr. After ZnO film deposition, electrical contact pad areas were patterned by photolithography and the ZnO was etched using a solution that consisted of phosphoric acid, acetic acid, and deionized water (1:1:30).

As shown in FIG. **7**D, the partially completed biofilm sensor **200** was annealed at 800° C. for one hour to increase the resistivity of the ZnO [43]. After annealing, the resistance measured in the IDT increased from 150Ω to 30-40 MΩ. As compared to FIG. **7**C, there are generally no dimensional changes for the piezoelectric layer **160**, the electrode pattern **105** or the transducer mounting structure **35** as a result of the annealing process.

FIG. **6** is a schematic illustration of a gas-based flow ALD process **400** to cause the passivation. FIG. **7**E is a schematic diagram of the passivation layer **170** deposited partially on the electrode pattern of FIGS. **7**B, **7**C and **7**D and on the piezoelectric layer **160** of FIGS. **7**C and **7**D. Referring now to FIG. **6** and FIG. **7**E, the ZnO surface **160***a* of the SAW sensor **200** may be passivated by depositing an Al_2O_3 film using atomic layer deposition (ALD. To deposit the passivation layer **170**, Al_2O_3 ALD thin films were fabricated at 150° C. in a flow-through chamber of a Beneq Model TFS-500 atomic layer deposition reactor system (available from Beneq Oy, Vantaa, Finland). As shown on the left side of FIG. **6**, trimethylaluminum (TMA) $Al_2(CH_3)_3$, originating as a liquid precursor (not shown) that is converted to a vapor at **402** was introduced into the ALD reactor (not shown) and formed a single layer of the TMA **404** on the ZnO layer **160**. In the center of FIG. **6**, the single layer of the TMA **404** is purged of unbound TMA vapor to become a purged single layer **406** of the TMA. As shown on the right side of FIG. **6**, water vapor (H_2O) **414** as the oxygen source was introduced into the ALD reactor and a covalent bonding between the TMA layer **406** and hydroxyl group of the water vapor **414** was established creating a single atomic layer of aluminum oxide **416** deposition. Each deposition cycle results in a 0.09 nm/cycle of deposition rate consistently. The single atomic layer of aluminum oxide Al_2O_3 **416** thus becomes the passivation layer **170**. To illustrate that the TMA layer **406** has bonded with the hydroxyl group of the water vapor **414**, the size of the circles representing the aluminum oxide Al_2O_3 **416** are shown to be larger than the size of the circles representing the TMA layer **406**.

In view of the foregoing, those skilled in the art will understand that embodiments of the present disclosure relate to a surface acoustic wave (SAW) biofilm sensor **200** that includes SAW transducer **105**, piezoelectric film layer **160**, and passivation film layer **170**. The piezoelectric film layer **160** is

mounted over the SAW transducer **105** and the passivation film layer **170** is mounted over the piezoelectric film layer **160**. In one embodiment, the passivation layer **170** includes aluminum oxide, Al_2O_3. In yet another embodiment, the passivation layer **170** defines a thickness h of at least nanometers (nm). In a still further embodiment, the piezoelectric layer **160** includes zinc oxide, ZnO. In yet another embodiment, the piezoelectric layer **160** defines a thickness d of at least 40 nanometers (nm).

Further, in view of the foregoing, those skilled in the art will understand that embodiments of the present disclosure relate to a method of assembling a biofilm surface acoustic wave (SAW) sensor, e.g., biofilm SAW sensor **200**, that includes depositing a piezoelectric layer, e.g., piezoelectric layer **160**, on a SAW transducer electrode pattern, e.g., IDT electrode pattern **105**, and depositing a passivation layer, e.g., passivation layer **170**, on the piezoelectric layer **160**. The depositing a piezoelectric layer may include depositing a layer of zinc oxide ZnO on the SAW transducer electrode pattern **105**. In one embodiment, the depositing a layer of zinc oxide ZnO on the SAW transducer electrode pattern **105** may include depositing a layer of zinc oxide ZnO having a thickness d of at least 40 nanometers (nm).

Further, the depositing a passivation layer, e.g., passivation layer **170**, on the piezoelectric layer, e.g., piezoelectric layer **160**, may include depositing a layer of aluminum oxide Al_2O_3 on the piezoelectric layer **160**. The depositing a layer of aluminum oxide Al_2O_3 on the piezoelectric layer includes depositing a layer of aluminum oxide Al_2O_3 having a thickness h of at least 45 nanometers (nm) on the piezoelectric layer.

Additionally, the method of assembling the SAW biofilm sensor **200** may further include depositing the SAW transducer electrode pattern, e.g., IDT electrode pattern **105**, on a piezoelectric SAW loss reduction film layer, e.g., piezoelectric SAW loss reduction film layer **30**.

The method of assembling may further include depositing the piezoelectric SAW loss reduction film layer, e.g., piezoelectric. SAW loss reduction film layer **30**, on a substrate, e.g. substrate **32**.

The step of depositing a piezoelectric layer, e.g., piezoelectric layer **160**, on a SAW transducer electrode pattern, e.g., IDT electrode pattern **105**, may include pulsed laser deposition. Additionally, the step of depositing a passivation layer, e.g., passivation layer **170**, on a piezoelectric layer, e.g., piezoelectric layer **160**, may include atomic layer deposition.

Device Characterization and Testing

Before the SAW sensor was used to measure biofilm growth, the performance of the passivation film was characterized using an optical microscope to inspect the surface of the ZnO layer after exposure to growth media. The results were used to optimize the film thickness and fabrication process. The sensitivity of the sensor was studied by loading the sensor surface with &ionized (DI) water since its viscosity is negligible. After these characterization studies, the sensor response was tested using *E. coli* static biofilm growth.

Al_2O_3 Film Characterization

Based on the theoretical modeling calculation presented previously and the results shown in FIG. **8**, Al_2O_3 was selected as a passivation film. Al_2O_3 films were deposited to thicknesses of 20 nm-45 nm by ALD to investigate the minimum required thickness for ZnO passivation. SAW sensors with four different thicknesses (20 nm, 30 nm, 40 nm, and 45 nm) of ALD Al_2O_3 film were placed in a LB media bacterial suspension for two days. The surface of the device was inspected using optical microscopy. As shown in FIGS. **9-12**, visible ZnO damage was observed when the thickness of ALD Al_2O_3 was thinner than 45 nm.

More particularly, FIG. **9** is an optical microscopy image of a SAW biofilm sensor assembled in accordance with FIGS. **2-7**E passivated by ALD of Al_2O_3 with a passivation layer thickness of 20 nm showing damaged areas. FIG. **10** is an optical microscopy image of another SAW biofilm sensor assembled in accordance with FIGS. **2-7**E passivated by ALD of Al_2O_3 with a passivation layer thickness of 30 nm showing damaged areas. FIG. **11** is an optical microscopy image of yet another SAW biofilm sensor assembled in accordance with FIGS. **2-7**E passivated by ALD of Al_2O_3 with a passivation layer thickness of 40 nm showing damaged areas. Finally, FIG. **12** is an optical microscopy image of another SAW biofilm sensor assembled in accordance with FIGS. **2-7**E passivated by ALD of Al_2O_3 with a passivation layer thickness of 45 nm showing no damage.

Based on these experiments, the minimum required thickness of ALD Al_2O_3 film for the passivation of ZnO was 45 nm. Since thicker passivation films caused a high loss of sensitivity due to more initial mass loading, the 45 nm thick Al_2O_3 film was selected to passivate the SAW sensor.

In addition to ALD, other Al_2O_3 film deposition methods were investigated in order to evaluate the dependence of passivation layer performance on the fabrication process. E-beam evaporation and RF-sputtering were used to deposit 45 nm of Al_2O_3 film. However, after two days in an LB media bacterial suspension, these two passivation films were not able to protect the ZnO layer as shown in FIGS. **13-15**.

More particularly, FIG. **13** is an optical surface image of another SAW biofilm sensor **200** assembled in accordance with FIGS. **2-7**E passivated by a 45 nm Al_2O_3 film using e-beam evaporation showing damage. FIG. **14** is an optical surface image of still another SAW biofilm sensor **200** assembled in accordance with FIGS. **2-7**E passivated by a 45 nm Al_2O_3 film using RF sputtering showing damage. FIG. **15** is an optical surface image of yet another SAW biofilm sensor **200** assembled in accordance with FIGS. **2-7**E passivated by a 45 nm Al_2O_3 film using ALD showing no damage.

This result can be due to non-uniform or lower density film deposition of IE-beam evaporation and RF-sputtering as compared to ALD. Therefore, ALD is a highly advantageous fabrication process for effective passivation of the ZnO using Al_2O_3.

Passivated SAW Sensor Characterization

The mass sensitivity and detection limit of the SAW sensor were studied by loading 10 μl of deionized (DI) water onto the sensor. A volume of 10 μl was used since that was the minimum volume of DI water required to cover the area between the two IDTs of the sensor. By measuring the resonant frequency shift upon mass loading, the sensitivity of the SAW sensor was calculated based on equations (3) and (6). The mass detection limit of the sensor was also calculated using the equipment resolution and the sensitivity.

Real-Time Resonant Frequency Monitoring

As illustrated in FIG. **16**, for real time resonant frequency monitoring in bacterial biofilm formation experiments, a custom biofilm sensing package **500** was designed to enable low impedance Bayonet Neill-Concelman (BNC) cable connections for RF applications with a network analyzer (HP8510B, Agilent Inc. USA) (not shown). The device biofilm sensing package **500** includes a bacterial growth well **502**, which was used to prevent bacterial growth media leakage and localize the bacterial growth, and a chip package **504**, that includes two separate portions **5041** and **5042** on either longitudinal side of the SAW sensor **200** connecting the sensor input BNC cable **510** and sensor output BNC cable **512** and BNC cables

520 and 522 for generating RF radiation. The SAW sensor 200 was placed in the bacterial growth well 502 and connected to the BNC connectors 520 and 522 by lead soldering on the chip package 504. The network analyzer was used to sweep a wide range of RF frequencies into the sensor 200 and the device resonant frequency was analyzed using S-parameter analysis. The resonant frequency of the sensor 200 was detected by measuring a low peak of the reflective power ratio (S_{11}) in the network analyzer. Data was collected and saved to a computer (not shown) every minute using general purpose interface bus (GPIB) communication (not shown) with the network analyzer.

Biofilm Growth Experiments with the SAW Sensor

E. coli W3110 was cultured in a shaking incubator for about 16 hours. The grown bacterial suspension was diluted with LB media or 10% FBS to make the initial OD_{600} approximately 0.21-0.23. The total volume of the diluted bacterial suspension in the growth well 502 was 20 ml in experiments with both types of media. The FBS solution was prepared to a 10% concentration by diluting with Dulbecco/Vogt modified Eagle's minimal essential medium (Invitrogen Inc, USA). After filling the bacterial growth well 502 with the diluted bacterial suspension, the well was sealed by paraffin film to prevent evaporation of the media during the experiment. The package 500 was placed on a 37° C. hotplate 530, and a polystyrene container (not shown) covered the whole package to reduce the temperature gradient near the test setup. After each biofilm growth experiment, the sensor 200 was recalibrated using DI water loading. The thickness of biofilm was measured optically by the distance difference between the focal plane of the sensor surface and the focal plane of the top of any accumulated biofilm.

Results and Discussion

ZnO Film Characterization

The generation of Love mode SAW was confirmed by investigating the lattice orientation of the deposited ZnO thin film, X-ray diffraction (XRD) was employed for crystal structure characterization of the ZnO layer after PLD deposition on a SiO_2/Si substrate by measuring the diffraction angle (2θ). The diffraction angles of the in the ZnO film at 34.25° and 72.25°, corresponding to c-axis (002) and (004) lattice orientations, were the most intensive reflections in the PLD prepared ZnO film. This c-axis orientation of ZnO crystal lattice ((00L) direction) was perpendicular to the substrate so that the Love mode of SAW generation was dominant on the surface of the sensor [15-22].

Photoluminescence (PL) spectroscopy was used to investigate the crystal quality of the ZnO film. The peak wavelength of the emitted light was approximately 380 nm, corresponding to the characteristic ZnO bandgap energy (3.3 eV). Therefore, the PL spectroscopy result confirmed that the PLD-prepared ZnO film had a low number of impurities.

Biofilm Cleaning

Consecutive biofilm growth tests using the same device are essential to investigate the reliability and repeatable operation of the SAW sensor. To test the sensor over multiple biofilm growth experiments, surface cleaning after a biofilm growth experiment was crucial for subsequent biofilm growth; cleaning not only sterilized the sensor, but also prevented initial mass loading due to the uncleaned biofilm and the resulting significant loss of sensitivity. Oxygen plasma applied for 30 s at 150 W RF-power was successfully employed to clean any remaining biofilm as shown in FIGS. 17 and 18

FIG. 17 is an optical microscopy image of the surface of the SAW biofilm sensor 200 assembled in accordance with FIGS. 2-7E before biofilm cleaning.

FIG. 18 is an optical microscopy image of the surface of the SAW biofilm sensor 200 assembled in accordance with FIGS. 2-7E after oxygen plasma biofilm cleaning.

The 45 nm ALD Al_2O_3 film passivation and oxygen plasma biofilm cleaning method enable SAW sensor 200 to be reusable over consecutive biofilm growth experiments.

Sensor Sensitivity

The sensitivity and detection limit of the SAW sensor were studied and calculated by loading 10 μl of DI water on the sensor and monitoring the magnitude of the resonant frequency shift. After loading 10 si of DI water, the resonant frequency shift of the SAW sensor was measured to be about 188 KHz by the network analyzer. Hence, the sensitivity of the sensor was 1.88×10^{10} Hz/g. Based on the network analyzer resolution (0.1 Hz), the detection limit of the sensor (resolution/sensitivity) was approximately 5.3 pg (picograms). Since the mass of a bacterium is known to be approximately 1 pg [44], this detection limit validates the SAW sensor application for bacterial biofilm monitoring.

Biofilm Growth Experiments in the SAW Sensor

The resonant frequency shift results of the SAW sensor due to the biofilm growth in LB media and in 10% PBS are shown in FIGS. 19, 20 and 21.

FIG. 19 is a graphical plot of negative resonant frequency shift results the SAW biofilm sensors assembled in accordance with FIGS. 2-7E versus time due to lysogeny broth (LB) biofilm growth for three newly fabricated SAW transducers.

FIG. 20 is a graphical plot of negative resonant frequency shift results for a SAW biofilm sensor assembled in accordance with FIGS. 2-7E versus time due to lysogeny broth biofilm growth in three sequential growth experiments using one device in an LB.

FIG. 21 is a graphical plot of negative resonant frequency shift results for a SAW biofilm sensor assembled in accordance with FIGS. 2-7E versus time in three growth experiments using a newly fabricated sensor in 10% fetal bovine serum (FBS).

In nature, bacterial growth in hatch culture begins with a lag phase where bacteria are not dividing but are actively adapting to the culture conditions. After this period, bacteria divide at a fast rate during the exponential phase of growth. Eventually, once the reactor contains a high population density and a limited supply of nutrients, the culture reaches stationary phase [45].

FIG. 19 shows the resonant frequency shift results from three newly fabricated devices (device 1, 2, and 3) in the first biofilm growth experiment in LB media. The frequency shift results of each new sensor show exponential resonant frequency changes at the beginning without the preceding lag phase as compared to the natural bacterial growth trend. These output responses of the SAW sensor can be because the overnight cultured *E. coli* are in a metabolically active state. When active bacteria are diluted to the same growth media, the lag phase may not be observed because bacteria do not have to change their metabolism [46]. However, the stationary phase frequency shifts in LB media biofilm experiments are varied, i.e. 0.8 MHz, 2.3 MHz, and 4.1 MHz for each device.

FIG. 20 illustrates the results when one of the newly fabricated SAW sensors (device 2) after the first experiment of FIG. 19 was selected and used for two additional sequential biofilm growth experiments, i.e., (2nd) and (3rd) in LB media, compared to the biofilm growth experiment for Device 2 in FIG. 19, designated as (1st), with the oxygen plasma cleaning applied between uses. The frequency shift results of sequential biofilm growth experiments in LB media as shown in FIG.

20 correspond to an exponential growth at the beginning, but the frequency shift observed during stationary phase also varies from 1 MHz to 2.3 MHz. The detection limit of the SAW sensor after each sequential biofilm growth experiment was studied by loading 10 μl DI water on the sensor. The summary of the calculated detection limit of the SAW sensor for the consecutive experiments are shown in Table 1.

TABLE 1

Summary of the detection limit of the SAW sensor in sequential biofilm growth experiments.

	Before biofilm experiment	After 1st biofilm growth experiment	After 2nd biofilm growth experiment	After 3rd biofilm growth experiment
Frequency shift due to 10 μl DI water	185 kHz	157 kHz	141 kHz	143 kHz
Sensitivity	1.85×10^{10} Hz/g	1.57×10^{10} Hz/g	1.41×10^{10} Hz/g	1.43×10^{10} Hz/g
Detection limit	5.4 pg	6.4 pg	7.1 pg	7.0 pg

As shown in Table 1, the detection limit of the sensor changed minimally after consecutive biofilm growth experiments, demonstrating excellent sensitivity recovery of the sensor. Therefore, the large variance in the final resonant frequency shift seen in LB media is not a result of sensor degradation, but can be due to non-uniform growth of the biofilm based on the results shown in FIGS. **19** and **20** and in Table 1. To investigate the biofilm growth variance in LB media and in 10% FBS, twelve test devices were prepared and placed in a bacterial suspension prepared as previously described. The biofilm thickness was measured after two days at 30 to 40 locations on the devices using an optical microscope.

FIG. **22** is a graphical plot of averaged biofilm thickness and standard deviation in LB media and in 10% FBS over 30-40 locations measured by optical microscopy. As shown in FIG. **22**, the measured average biofilm thicknesses in LB media and in 10% FBS were 135 μm and 32 μm respectively.

The standard deviation of the measured biofilm thickness in LB media (62 μm, about 46% of the average biofilm thickness) was significantly more than the standard deviation in 10% FBS (6.4 μm, about 20% of average biofilm thickness).

These results correspond to the large growth variance in LB media measured by the resonant frequency shift of the SAW sensor. Based on these experimental biofilm growth variance results and the sensitivity characterization work as shown in Table 1, the stationary phase resonant frequency shift variation in LB media in FIGS. **19** and **20** can be attributed to the natural variation in biofilm growth. The LB media, which is a standard bacterial growth media, is composed of essential materials for *E. coli* growth, such as amino acids, yeast, and NaCl. Thus, the media can provide a favorable environment for biofilm growth. The 10% FBS is mainly composed of diverse blood proteins, such as globular protein and Bovine Serum Albumin (BSA), and has been widely used as a simulated in vivo condition for mammalian cell culture. These composition differences between in LB media and in 10% FBS will cause different bacterial growth rates in each media, contributing to the observed difference in biofilm thickness.

FIG. **21** illustrates the resonant frequency shift results in 10% FBS biofilm growth experiments. In 10% FBS tests, a newly fabricated SAW sensor was used in three consecutive bacterial biofilm growth experiments, using oxygen plasma cleaning between experiments. As shown in FIG. **21**, the frequency shift of the sensor also corresponds to exponential growth trend. Furthermore, the variation in the stationary phase in each experiment was only about 0.3 MHz which was much less than variation in LB media (about 3.3 MHz). This smaller difference in the final frequency shifts in 10% FBS compared to the LB media biofilm growth experiments can be due to the more uniform biofilm growth in 10% FBS as shown in FIG. **22**.

FIG. **23** is a microscopy image of a SAW biofilm sensor assembled in accordance with FIGS. **2**-**7**E after biofilm growth experiments in LB media;

FIG. **24** is a microscopy image of the SAW biofilm sensor of FIG. **23** assembled in accordance with FIGS. **2**-**7**F, after biofilm growth experiments in 10% FBS;

After biofilm growth experiments in each media, the presence of bacterial biofilm on the SAW sensor was confirmed by optical microscopy as shown images in FIGS. **23** and **24**.

As shown by the data, the 45 nm ALD Al_2O_3 passivated SAW sensor was able to measure biofilm growth repeatably using oxygen plasma cleaning between experiments. The final frequency shift results in LB media were more variable than those in 10% FBS since the composition of the LB media was a more favorable environment to *E. coli*, thereby indicating non-uniform biofilm growth in each experiment [47]. The observed SAW sensor outputs in both media followed the same growth trends. Moreover, the 10% FBS results suggest that the SAW sensor can be applied to in vivo biofilm detection in the future. Since the FBS is composed of blood proteins and plasma, the serum can be used to mimic an in vivo environment. The resonant frequency shift results of the SAW sensor in 10% HIS are more repeatable than results in LB media, rendering reliable operation of the sensor in an in vivo environment more likely. The effective passivation of the sensor using an ALD Al_2O_3 film also contributed to reliable sensing in 10% FBS.

FIG. **25** is a microscopy image of a SAW biofilm sensor, such as SAW biofilm sensor **200** assembled in accordance with FIGS. **2**-**7**E after cleaning with deionized water.

FIG. **26** is a microscopy image of the SAW biofilm sensor of FIG. **25** after ultrasonication cleaning in acetone for 3 hours.

FIG. **27** is a microscopy image of the SAW biofilm sensor of FIGS. **25** and **26** after oxygen plasma cleaning for 30 seconds.

FIG. **28** is a microscopy image of the SAW biofilm sensor of FIGS. **25**, **26** and **27** after a second biofilm growth experiment and oxygen plasma cleaning for 30 seconds.

The results indicated by FIGS. **25** to **28** illustrate that the SAW sensor **200** can be reused after oxygen plasma cleaning, allowing for consecutive biofilm formation experiments using one sensor.

In view of the foregoing description, those skilled in the art will understand and appreciate that a novel ALD Al_2O_3 film passivated SAW sensor for real time biofilm monitoring has been successfully demonstrated. A high quality c-axis ori-

ented ZnO film was deposited by PLD, and the sensor was effectively passivated by 45 nm of Al_2O_3 film using ALD to prevent ZnO damage in the bacterial growth media and animal serum. For the reliable passivation of the ZnO SAW sensor, ALD was an important fabrication method based on its highly dense and conformal film deposition capabilities. The SAW sensor can be reused after oxygen plasma cleaning, allowing for consecutive biofilm formation experiments using one sensor. The detection limit of the SAW sensor was approximately 5.3 pg. The resonant frequency shift results of the SAW sensor followed natural bacterial biofilm growth properties not only in LB media which provided a favorable bacterial growth environment, but also in 10% FBS as a simulated in vivo environment. These results validate the application of the SAW sensor for real-time bacterial growth monitoring.

FIG. **29** is a perspective view a top perspective view of an exemplary embodiment of a SAW biofilm sensor **600** disposed on a substrate **610**. The SAW biofilm sensor **600** includes an IDT **602** and an RF reflective tag **604** each disposed on the substrate **610** on an opposite side of a biofilm **40** such that a transmitted SAW **614** originating from the IDT **602** is reflected by the reflective tag **604** as a reflected SAW **616** back to the IDT **602**. The IDT **602** senses the reflected SAW **616** and via an antenna **606** in RF coupling **612** to an RF reader **608** to enable remote biofilm growth detection.

This SAW sensor **600** combined with RF wireless communication techniques can be used to detect in vivo biofilm growth, which is the groundwork for developing an implantable sensor for early biofilm detection and prevention of major infections.

Although the present disclosure has been described in considerable detail with reference to certain preferred version thereof, other versions are possible and contemplated. Therefore, the spirit and scope of the appended claims should not be limited to the description of the preferred versions contained therein.

Any element in a claim that does not explicitly state "means for" performing a specified function or "step for" performing a specified function, is not to be interpreted as a "means" or "step" clause as specified in 35 U.S.C. §112, ¶6. In particular, the use of "step of" in the claims is not intended to invoke the provisions of 35 U.S.C. §112, ¶6.

While several embodiments of the disclosure have been shown in the drawings, it is not intended that the disclosure be limited thereto, as it is intended that the disclosure be as broad in scope as the art will allow and that the specification be read likewise. Therefore, the above description should not be construed as limiting, but merely as exemplifications of particular embodiments. Those skilled in the art will envision other modifications within the scope of the claims appended hereto.

In the claims, any reference signs placed between parentheses shall not be construed as limiting the claim. The word "comprising" does not exclude the presence of elements or steps other than those listed in a claim. The word "a" or "an" preceding an element does not exclude the presence of a plurality of such elements. The embodiments of the present disclosure may be implemented by means of hardware comprising several distinct elements, and/or by means of a suitably programmed processor. In the device claim enumerating several means, several of these means may be embodied by one and the same item of hardware. The mere fact that certain measures are recited in mutually different dependent claims does not indicate that a combination of these measures cannot be used to advantage.

REFERENCES

The entire contents and teachings of the following references are incorporated herein by reference.

These references are identified as source documents for the particular portion of the foregoing description by indication of the number or numbers in parentheses [1]-[47] corresponding to one or more of the references below.

[1] J. W. C, Philip S. Stewart, E. P. Greenberg, Bacterial Biofilms: A Common Cause of Persistent infections, SCIENCE, VOL 284, (1999), p. 1318-1322,

[2] Sutherland, I. W., Bacterial exopolysaccharides their nature and production, Surface Carbohydrates of the Prokaryotic Cell, London, Academic Press, (1977), p. 27-96.

[3] J. W. Costerton, Z. Lewandowski, D. E Caldwell, D. R. Corber, H. M. Lappin-Scott, Bacterial biofilms in nature and disease, Annu. Rev. Microbiol, 41, (1987), p. 435-506.

[4] Liju Yang, and Yanbin Li, Detection of viable *Salmonella* using microelectrode-based capacitance measurement coupled with immunomagnetic separation, J MICROBIOL METH, 64, (2006), p. 9-16.

[5] Ebrahim Ghafar-Zadeh, Mohamad Sawan, Vamsy P. Chodavarapu, and Tahereh Hosseini-Nia, Bacteria Growth Monitoring Through a Differential CMOS Capacitive Sensor, IEEE T BIO-MED ENG, VOL. 4, NO. 4, (2010), p. 232-238.

[6] X. Munoz-Berbel, N. Vigues, A. T. A. Jenkins, J. Mas, F. J. Munoz, Impedimetric approach for qualifying low bacteria concentrations based on the changes produced in the electrode-solution interface during the pre-attachment stage, Biosens. Bioelectron., 23, (2008), p. 1540-1546.

[7] E. Spiller, A. Scholl, R. Alexy, K. Kummerer, G. A. Urban, A sensitive microsystem as biosensor for cell growth monitoring and antibiotic testing, Sensor Actuat A, 130-131, (2006), p. 312-321.

[8] Ewa Heyduk, Tomasz Heyduk, Fluorescent homogeneous immunosensors for detecting pathogenic bacteria, Anal. Biochem., (2010), p. 396, 298-303.

[9] Benjamin J. Privett, Jae Ho Shin, and Mark H. Schoenfisch, Electrochemical Sensors, Anal. Chem., 82, (2010), p. 4723-4741.

[10] Michiel van Leeuwen, Erik E. Krommenhoek, Joseph J. Heijnen, Han Gardeniers, Luuk A. M. van der Wielen and Walter M. Van Gulik, Aerobic Batch Cultivation in Micro Bioreactor with integrated Electrochemical Sensor Array, Biotechnol, Prog., Vol. 26, No. 1, (2010), p. 293-300.

[11] G. L. Harding, J. Du, P. R. Dencher, D. Barnett, E. Howe, Love wave acoustic immunosensor operating in liquid, Sens. Actuat A, 61, (1997), p. 279-286.

[12] J. Du, G. L. Harding, J. A. Ogilvy, P. R. Dencher, M. Lake, A study of Love-wave acoustic sensors, Sens. Actuat. A, 56, (1996), p. 211-219.

[13] J. Du, G. L. Harding, A. F. Collings, P. R. Dencher, An experimental study of Love-wave acoustic sensors operating in liquids, Sens. Actuat. A, 60, (1997), p. 54-61.

[14] K. Z. Kourosh, W. Wlodarskia, Y. Y. Chene, B. N. Frye, K. Galatsisa, Novel Love mode surface acoustic wave based immunosensors, Sens. Actuat B, 91, (2003), p. 143-147.

[15] S. Krishnamoorthy, A. A. Iliadis, Properties of high sensitivity ZnO surface acoustic wave sensors on SiO_2/(100) Si substrates, Solid-State Electron., 52, (2008), p. 1710-1716.

[16] H. Morkoc and U. Ozgur, Zinc Oxide: Fundamentals, Materials, and Device Technology (Chapter 1: General Properties of ZnO), WILEY-VCH Verag GmbH, Weinheim, 2009.

[17] R. D. Vispute et al., High quality crystalline ZnO buffer layers on sapphire (001) by pulsed laser deposition for III-V nitrides, Appl. Phys. Lett. 70 (20), (1997), p. 2735-2737.

[18] S. Krishnamoorthy, A. A. Iliadis, Development of high frequency ZnO/SiO2/Si Love mode surface acoustic wave devices, Solid-State Electron., 50, (2006), p. 1113-1118.

[19] S. Krishnamoorthy, A. A. Iliadis, Thaleia Bei, George P. Chrousos, An interleukin-6 ZnO/SiO2/Si surface acoustic wave biosensor, BIOSENS BIOELECTRON, 24, (2008), p. 313-318.

[20] M. C. Horrillo et al., Optimization of SAW sensors with a structure ZnO—SiO2-Si to detect volatile organic compounds, Sens. Actuat. B, 118, (2006), p. 356361, 2006.

[21] X. Chen, D. Liu, Temperature stability of ZnO-based Love wave biosensor with SiO2 buffer layer, Sens. Actuat. A, 156, (2009), p. 317-322.

[22] X. Chen, D. Liu, J. Chen, G. Wang, The effect of a SiO2 layer on the performance of a ZnO-based SAW device for high sensitivity biosensor applications, Smart Mater. Struct. 18, (2009), 115021.

[23] A. Springer, R. Weigel, A. Pohl, F. Seifert, Wireless identification and sensing using surface acoustic wave devices, IEEE ASME Trans Mechatron, 9, (1999), p. 745-756.

[24] Alfred Pohl, A Review of Wireless SAW Sensors, IEEE Trans Ultrason Ferroelectr Freq Control, Vol. 47, No. 2, (2000), p. 317-332.

[25] Arruda David L, Wilson William C, Nguyen Crystal, Yao Qi W, Caiazzo Robert, Talpasanu Ilie, Microelectrical sensors as emerging platforms for protein biomaker detection in point-of-care diagnostic, Expert Rev. of Mol. Diagn., Vol. 9, No. 7, (2009), p. 749-755.

[26] M. Bisoffi, Detection of viral bioagents using a shear horizontal surface acoustic wave biosensor, BIOSENS BIOELECTRON, 23, (2008), pp. 1397-1403.

[27] Y. Q. Fu, J. K. Luo, X. Y. Du, A. J. Hewitt, Y. Li, G. H. Markx, Recent developments on ZnO films for acoustic wave bio-sensing and microfluidic applications: a review, SENSOR ACTUAT B-CHEM, 143, (2010), p. 606-619.

[28] Irie R F, Natural antibody in human serum to neoantigen in human cultured cells grown in fetal bovine serum, J. Natl Cancer Inst. 52(4), (1974), p. 1051-1058.

[29] Glen McHale, Generalized concept of shear horizontal acoustic plate mode and Love wave sensors, Meas. Sci Technol. 14, (2003), p. 1847-1853.

[30] Biljana A. Cavic, Gordon L. Hayward, and Michael Thompson, Acoustic waves and the study of biochemical macromolecules and cells at the sensor-liquid interface, Analyst, 124, (1999), p. 1405-1420

[31] Bill Drafts, Acoustic Wave Technology Sensors, IEEE T MICROW THEORY, Vol. 49, No. 4, (2001), p. 795-802.

[32] Federal Communications Commission, Title 47 C.F.R., Chapter I, Subchapter D, Part 95, Subpart I, paragraph 1209, "Permissible communications", 77 FR 55733, as amended through Sep. 11, 2012.

[33] Douglas H. Lowndes, D. B. Geohegan, A. A. Puretzky, D. P. Norton, C. M. Rouleau, Synthesis of Novel Thin-Film Materials by Pulsed Lase Deposition, Science, VOL 273, (1996), p. 898-903.

[34] Susan E. Voss and Jont B. Allen, Measurement of acoustic impedance and feflectance in the human ear canal, J. Acoust. Soc. Am, 95 (1), (1994), p. 372-384.

[35] B. Jakoby, M. J. Vellekoop, Properties of Love waves: application in sensors, Smart Mater. Struct. 6, (1997), p. 668-679.

[36] J. Su, Z. B. Kuang, H. Liu, Love wave in ZnO/SiO2/Si structure with initial stresses, Journal of Sound and Vibration, 286, (2005), p. 981-999.

[37] R. C. Chang, S. Y. Chu, C. S. Hong, Y. T. Chuang, A study of Love wave devices in ZnO/Quartz and ZnO/LitaO3 structures, Thin Solid Films, 498, (2006), 146-151.

[38] W. C. Shih, H. Y. Su, M. S. Wu, Deposition of ZnO thin films on SiO2/Si substrate with Al2O3 buffer layer by radio frequency magnetron sputtering for high frequency surface acoustic wave devices, Thin Solid Films, 517, (2009), p. 3378-3381.

[39] W. C. Shih, T. L. Wang L. L. Hsu, Surface acoustic wave properties of aluminum oxide films on lithium niobate, Thin Solid Films, 518, (2010), p. 7143-7146.

[40] J. Du, G. L. Harding, A multilayer structure for Love-mode acoustic sensors, Sens, Actuat A, 65, (1998), p. 152-159.

[41] NIST Property Data Summaries, http://www.ceramics.nist.gov/srd/summary/emodox00.htm

[42] http://www.lenntech.com/teflon.htm, http://www.cct-plastics.com/teflonall.html

[43] Hang-Ju Ko, Myung-Soo Han, Young-Sik Park, Yun-Sik Yu, Byoung-In Kim, Sang Sub Kim, Improvement of the quality of ZnO substrates by annealing, J of Cryst Growth, 269, (2004), p. 493-498.

[44] Davis, Dulbecco, Eisen, Ginsberg, *Bacterial Physiology: Microbiology, Second Edition*, Maryland: Harper and Row, (1973), p. 96-97.

[45] Jeffrey V. Straight and Doraiswami Ramkrishna, Modeling of Bacterial Growth under Multiply-Limiting Conditions, Experiments under Carbon- or/and Nitrogen-Limiting Conditions, Biotechnol. Prog. 10, (1994), p. 588-605.

[46] Augustin J. C. et al., Significance of Inoculum Size in the Lag Time of *Listeria monocytogenes*, APPL. ENVION. MICROBIOL. Vol. 66, (2000), p. 1706-1710.

[47] Mariana T Meyer, Varnika Roy, William E Bentley, and Reza Ghodssi, Development and validation of a microfluidic reactor for biofilm monitoring via optical methods, J. Micromech. Microeng., 21, (2011), 054023.

[48] Federal Communications Commission, Title 47 C.F.R., Chapter I, Subchapter D, Part 95, Subpart E, paragraph 627, "MedRadio transmitters in the 401-406 MHz band", as amended through 77 FR 4268, Jan. 27, 2012.

What is claimed is:

1. A method of passivating a surface acoustic wave sensor (SAW) using atomic layer deposition (ALD), comprising:

depositing on a zinc oxide (ZnO) surface of a SAW sensor in an ALD reactor an aluminum oxide (Al_2O_3) film;

introducing vaporized trimethylaluminum (TMA) $Al_2(CH_3)_3$ into the ALD reactor;

forming a single layer of the TMA on the ZnO surface;

purging the single layer of the TMA of unbound TMA vapor to become a purged single layer of the TMA; and

introducing water vapor into the ALD reactor to create a single atomic layer of aluminum oxide deposition as a passivation layer of the SAW sensor.

2. The method according to claim **1**, further comprising,

prior to introducing vaporized trimethylaluminum (TMA) $Al_2(CH_3)_3$ into the ALD reactor,

fabricating a liquid precursor of trimethylaluminum (TMA) $Al_2(CH_3)_3$.

3. The method according to claim **2**, further comprising,

prior to introducing vaporized trimethylaluminum (TMA) $Al_2(CH_3)_3$ into the ALD reactor and after fabricating a liquid precursor of trimethylaluminum (TMA) $Al_2(CH_3)_3$,

converting the liquid precursor to a vapor.

4. The method according to claim **1**, further comprising:

maintaining temperature inside the ALD reactor at 150 degrees Celsius.

5. The method according to claim 1, wherein the creating a single atomic layer of aluminum oxide deposition as a passivation layer of the SAW sensor occurs at a deposition cycle rate of 0.09 nanometers per cycle.

6. The method according to claim 1, further comprising:

depositing a layer of zinc oxide ZnO to provide the ZnO surface on the SAW sensor.

7. The method according to claim 6, wherein the depositing of a layer of zinc oxide ZnO as the surface as the ZnO surface on the SAW sensor includes depositing the layer of zinc oxide ZnO having a thickness of at least 40 nanometers (nm).

8. The method according to claim 6, wherein the depositing of a layer of zinc oxide ZnO as the surface as the ZnO surface on the SAW sensor includes depositing the layer of zinc oxide ZnO having a thickness of at least 45 nanometers (nm).

9. The method according to claim 1, wherein the passivation layer of the SAW sensor is deposited on a SAW transducer electrode pattern of the SAW sensor.

10. A system for passivating a surface acoustic wave sensor (SAW) using atomic layer deposition (ALD), comprising:

an atomic layer deposition (ALD) reactor configured to receive a SAW sensor, the SAW sensor including as a piezoelectric layer a zinc oxide (ZnO) surface,

the system at least configured to execute one or more actions to, or at least configured to enable a user to:

deposit on the zinc oxide (ZnO) surface of the SAW sensor received in the ALD reactor an aluminum oxide (Al_2O_3) film;

introduce vaporized trimethylaluminum (TMA) $Al_2(CH_3)_3$ into the ALD reactor;

form a single layer of the TMA on the ZnO surface;

purge the single layer of the TMA of unbound TMA vapor to become a purged single layer of the TMA; and

introduce water vapor into the ALD reactor to create a single atomic layer of aluminum oxide deposition as a passivation film layer of the SAW sensor.

11. The system according to claim 10, wherein the system is configured to execute one or more actions to, or is configured to enable a user to:

prior to introducing vaporized trimethylaluminum (TMA) $Al_2(CH_3)_3$ into the ALD reactor,

fabricate a liquid precursor of trimethylaluminum (TMA) $Al_2(CH_3)_3$.

12. The system according to claim 11, wherein the system is configured to execute one or more actions to, or is configured to enable a user to:

prior to introducing vaporized trimethylaluminum (TMA) $Al_2(CH_3)_3$ into the ALD reactor and after fabricating a liquid precursor of trimethylaluminum (TMA) $Al_2(CH_3)_3$,

convert the liquid precursor to a vapor.

13. The system according to claim 10, wherein the system is configured to execute one or more actions to, or is configured to enable a user to:

maintain temperature inside the ALD reactor at 150 degrees Celsius.

14. The system according to claim 10, wherein the system is configured to execute one or more actions such that, or is configured to enable a user such that:

the creating of a single atomic layer of aluminum oxide deposition as a passivation film layer of the SAW sensor occurs at a deposition cycle rate of 0.09 nanometers per cycle.

15. The system according to claim 10, wherein the system is configured to execute one or more actions to, or is configured to enable a user to:

deposit a layer of zinc oxide ZnO as the ZnO surface on the SAW sensor.

16. The system according to claim 15, wherein the system is configured to execute one or more actions such that, or is configured to enable a user such that, the depositing of a layer of zinc oxide ZnO as the surface as the ZnO surface on the SAW sensor includes depositing the layer of zinc oxide ZnO having a thickness of at least 40 nanometers (nm).

17. The system according to claim 15, wherein the system is configured to execute one or more actions such that, or is configured to enable a user such that, the depositing of a layer of zinc oxide ZnO as the surface as the ZnO surface on the SAW sensor includes depositing the layer of zinc oxide ZnO having a thickness of at least 45 nanometers (nm).

18. The system according to claim 10, wherein the system is configured to execute one or more actions such that, or is configured to enable a user such that, the passivation film layer of the SAW sensor is deposited on a SAW transducer electrode pattern of the SAW sensor.

19. A surface acoustic wave (SAW) biofilm sensor comprising:

a SAW transducer;

a piezoelectric film layer; and

a passivation film layer,

the piezoelectric film layer mounted over the SAW transducer and the passivation film layer mounted over the piezoelectric film layer,

the SAW biofilm sensor manufactured by a method of using atomic layer deposition (ALD), comprising:

depositing on a zinc oxide (ZnO) surface of the SAW biofilm sensor in an ALD reactor an aluminum oxide (Al_2O_3) film;

introducing vaporized trimethylaluminum (TMA) $Al_2(CH_3)_3$ into the ALD reactor;

forming a single layer of the TMA on the ZnO surface;

purging the single layer of the TMA of unbound TMA vapor to become a purged single layer of the TMA; and

introducing water vapor into the ALD reactor to create a single atomic layer of aluminum oxide deposition as the passivation layer of the SAW biofilm sensor.

20. The SAW biofilm sensor according to claim 19, wherein the method of using atomic layer deposition (ALD) further comprises:

prior to introducing vaporized trimethylaluminum (TMA) $Al_2(CH_3)_3$ into the ALD reactor,

fabricating a liquid precursor of trimethylaluminum (TMA) $Al_2(CH_3)_3$.

21. The SAW biofilm sensor according to claim 20, wherein the method of using atomic layer deposition (ALD) further comprises:

prior to introducing vaporized trimethylaluminum (TMA) $Al_2(CH_3)_3$ into the ALD reactor and after fabricating a liquid precursor of trimethylaluminum (TMA) $Al_2(CH_3)_3$,

converting the liquid precursor to a vapor.

22. The SAW biofilm sensor according to claim 19, wherein the method of using atomic layer deposition (ALD) includes wherein the

depositing on a zinc oxide (ZnO) surface of the SAW biofilm sensor in an ALD reactor an aluminum oxide (Al_2O_3) film includes the zinc oxide (ZnO) surface of the SAW biofilm sensor being a zinc oxide (ZnO) surface of a zinc oxide (ZnO) piezoelectric film layer that is the piezoelectric film layer of the SAW biofilm sensor.

23. The SAW biofilm sensor according to claim 19, wherein the method of using atomic layer deposition (ALD) includes wherein the depositing of a layer of zinc oxide ZnO

as the surface as the ZnO surface on the SAW sensor includes depositing the layer of zinc oxide ZnO having a thickness of at least 40 nanometers (nm).

24. The SAW biofilm sensor according to claim **19**, wherein the method of using atomic layer deposition (ALD) includes wherein the depositing of a layer of zinc oxide ZnO as the surface as the ZnO surface on the SAW sensor includes depositing the layer of zinc oxide ZnO having a thickness of at least 45 nanometers (nm).

25. The SAW biofilm sensor according to claim **19**, wherein the method of using atomic layer deposition (ALD) includes the creating of a single atomic layer of aluminum oxide deposition as a passivation layer of the SAW sensor occurring at a deposition cycle rate of 0.09 nanometers per cycle.

26. A surface acoustic wave (SAW) biofilm sensor comprising:

a first transducer defining an upper surface and a lower surface;

a second transducer defining an upper surface and a lower surface;

a piezoelectric film layer defining an upper surface and a lower surface; and

a passivation film layer defining an upper surface and a lower surface,

a portion of the lower surface of the piezoelectric film layer disposed on the upper surface of the first transducer,

another portion of the lower surface of the piezoelectric film layer disposed on the upper surface of the second transducer, and

the lower surface of the passivation film layer disposed on the upper surface of the piezoelectric film layer,

the upper surface of the passivation film layer configured thereby to enable contact with a biofilm,

the SAW biofilm sensor manufactured by a method of using atomic layer deposition (ALD), comprising:

depositing on a zinc oxide (ZnO) surface of the SAW biofilm sensor in an ALD reactor an aluminum oxide (Al_2O_3) film;

introducing vaporized trimethylaluminum (TMA) $Al_2(CH_3)_3$ into the ALD reactor;

forming a single layer of the TMA on the ZnO surface;

purging the single layer of the TMA of unbound TMA vapor to become a purged single layer of the TMA; and

introducing water vapor into the ALD reactor to create a single atomic layer of aluminum oxide deposition as the passivation film layer of the SAW biofilm sensor.

27. The SAW biofilm sensor according to claim **26**, the SAW biofilm sensor further comprising:

a piezoelectric SAW loss reduction film layer defining an upper surface and a lower surface

wherein the lower surface of the first transducer is disposed on a portion of the upper surface of the piezoelectric SAW loss reduction film layer and

wherein the lower surface of the second transducer is disposed on another portion of the upper surface of the piezoelectric SAW loss reduction film layer.

28. The SAW biofilm sensor according to claim **27**, further comprising:

a substrate defining an upper surface and a lower surface,

wherein the lower surface of the piezoelectric SAW loss reduction film layer is disposed on the upper surface of the substrate.

29. The SAW biofilm sensor according to claim **27**, wherein

a portion of the lower surface of the piezoelectric film layer is disposed on a portion of the upper surface of the piezoelectric SAW loss reduction film layer and disposed between the first transducer and the receiving acoustic wave to electric transducer.

30. The SAW biofilm sensor according to claim **26**, wherein another portion of the lower surface of the piezoelectric film layer is disposed between the first transducer and the second transducer.

31. The SAW biofilm sensor according to claim **30**, wherein the piezoelectric layer defines an upper sub-layer and a lower sub-layer,

the lower sub-layer defined by the portion of the lower surface of the piezoelectric film layer disposed on the portion of the upper surface of the lower piezoelectric film layer and disposed between the first transducer and the second transducer,

the upper sub-layer defined by the portion of the piezoelectric film layer between the passivation film layer and the lower sub-layer,

the lower sub-layer having a shear modulus and density to define a first SAW velocity,

the upper sub-layer having a shear modulus and density to define a second SAW velocity wherein the second velocity differs from the first velocity.

32. The SAW biofilm sensor according to claim **30**, wherein the piezoelectric film layer defines an upper sub-layer and a lower sub-layer,

the lower sub-layer defined by the portion of the lower surface of the piezoelectric film layer disposed on the portion of the upper surface of the lower piezoelectric film layer and disposed between the first transducer and the second transducer,

the upper sub-layer defined by the portion of the piezoelectric film layer between the passivation film layer and the lower sub-layer,

the lower sub-layer having a shear modulus and density to define a first SAW velocity,

the upper sub-layer having a shear modulus and density to define a second SAW velocity wherein the second velocity is equal to or greater than the first velocity.

33. The SAW biofilm sensor according to claim **26**, wherein the passivation layer includes aluminum oxide, Al_2O_3.

34. The SAW biofilm sensor according to claim **33**, wherein the passivation film layer defines a thickness between the upper surface of the passivation film layer and the lower surface of the passivation film layer, the thickness of the passivation film layer having a dimension of at least 45 nanometers (nm).

35. The SAW biofilm sensor according to claim **33**, wherein the piezoelectric film layer includes zinc oxide, ZnO.

36. The SAW biofilm sensor according to claim **35**, wherein the piezoelectric film layer defines a thickness between the upper surface of the piezoelectric film layer and the lower surface of the piezoelectric film layer, the thickness of the piezoelectric film layer having a dimension of at least 40 nanometers (nm).

37. The SAW biofilm sensor according to claim **34**, wherein the piezoelectric film layer includes zinc oxide, ZnO.

38. The SAW biofilm sensor according to claim **37**,

wherein the piezoelectric film layer defines a thickness between the upper surface of the piezoelectric film layer and the lower surface of the piezoelectric film layer, the thickness of the piezoelectric film layer having a dimension of at least 40 nanometers (nm).

39. The SAW biofilm sensor according to claim **37**,

wherein the first transducer is a transmitting electric to acoustic wave transducer defining the upper surface and the lower surface of the first transducer; and

wherein the second transducer is a receiving acoustic wave to electric transducer defining the upper surface and the lower surface of the second transducer.

* * * * *